Marquette University
e-Publications@Marquette

Master's Theses (2009 -)   Dissertations, Theses, and Professional Projects

Capillary Perfusion Kinematics in Lungs of Oxygen-Tolerant Rats

Madhavi Ramakrishna
Marquette University

CAPILLARY PERFUSION KINEMATICS IN LUNGS OF OXYGEN–TOLERANT RATS

by

Madhavi Ramakrishna, B.E.

A Thesis submitted to the Faculty of the Graduate School,
Marquette University,
in Partial Fulfillment of the Requirements for
the Degree of Master of Science

Milwaukee, Wisconsin

December 2009

ABSTRACT
CAPILLARY PERFUSION KINEMATICS IN
LUNGS OF OXYGEN–TOLERANT RATS

Madhavi Ramakrishna, B.E.

Marquette University, 2009

Motivation:

Prolonged exposure to oxygen at high concentrations (hyperoxia), a common treatment for hypoxemia, is toxic to the lungs. Rats exposed to 85% O_2 for 5-7 days develop tolerance to the otherwise lethal effects of 100% O_2. Elucidating the factors that contribute to this tolerance could further our understanding of the mechanisms of lung O_2 toxicity. Since vascular remodeling involving loss of capillary volume and endothelial surface area has been reported in lungs from rats exposed to 85% O_2 for 7 days, we were interested in evaluating the effect of this hyperoxia model on lung capillary perfusion kinematics. This information is needed for evaluating the effect of this hyperoxia model on the metabolic functions of the pulmonary capillary endothelium, a primary target of O_2 toxicity. Thus, the objective was to evaluate the effect of this hyperoxia model on lung capillary mean transit time ($\bar{t}_c$) and distribution of capillary transit times ($h_c(t)$).

Methods:

Venous concentration versus time outflow curves of fluorescein isothiocyanate labeled dextran (FITC-dex), a vascular indicator, and coenzyme Q_1 hydroquinone (CoQ_1H_2), a compound which rapidly equilibrates with lung tissue on passage through the lung, were measured following their bolus injections into the pulmonary artery of isolated lungs from rats exposed to either room air or 85% O_2 for 7 days. A capillary surface area index was estimated by measuring the rate of hydrolysis of the angiotensin converting enzyme substrate N-[3-(2-Furyl) acryloyl]-Phe-Gly-Gly (FAPGG) on passage through each lung. The mean transit time and variance of the measured FITC-dex and CoQ_1H_2 curves were first determined and then used in a mathematical model to estimate $\bar{t}_c$ and the relative dispersion (RD_c) of $h_c(t)$.

Results:

FITC-dex and CoQ_1H_2 data revealed that hyperoxia decreased lung $\bar{t}_c$ by 41% and increased RD_c, a measure of the heterogeneity of $h_c(t)$, by 40%. FAPGG data revealed that hyperoxia decreased lung capillary surface area by 56%.

Conclusion:

This study demonstrates the utility of CoQ_1H_2 for evaluating the effect of hyperoxia on capillary perfusion kinematics in intact rat lungs. The results are important for subsequent evaluation of the effect of hyperoxia on the metabolic functions of the pulmonary capillary endothelium.

ACKNOWLEDGMENTS

Madhavi Ramakrishna, B.E.

TABLE OF CONTENTS

LIST OF TABLES

LIST OF FIGURES

1. INTRODUCTION AND BACKGROUND

1.1   Introduction

The most common initial treatment for hypoxemia in premature babies with respiratory distress syndrome, and adults with pulmonary insufficiency (e.g., acute respiratory distress syndrome (ARDS), pneumonia), is oxygen therapy (normobaric hyperoxia) (Jackson 1985; Singh 2001). However, exposure to high O_2 concentrations ($> 60\%$) for prolonged periods has been found to be toxic, primarily to the lungs (Bhandari et al. 2006; Crapo and Tierney 1974; Fisher and Beers 2008; Frank et al. 1989; Valenca Sdos et al. 2007). Although the mechanisms leading up to lung O_2 toxicity are not fully understood, there is ample evidence that the deleterious effects of high O_2 are the result of increased formation of reactive oxygen species (ROS), such as superoxide and hydrogen peroxide, which at high concentrations are known to cause various cytotoxic effects (Fisher 1987; Freeman and Crapo 1982; Freeman, Topolosky, and Crapo 1982; Heffner and Repine 1989; Jamieson et al. 1986; Kwak, Kwak, and Gauda 2006; Turrens et al. 1982).

Several animal models have been developed to investigate the underlying mechanisms of lung O_2 toxicity because of the clinical relevance of hyperoxic exposure and its importance as a model of oxidant-induced acute lung injury (Crapo et al. 1980; Crapo and Tierney 1974; Freeman, Topolosky, and Crapo 1982; Matute-Bello, Frevert, and Martin 2008; Valenca Sdos et al. 2007; Ware 2000). The rat model of hyperoxic lung injury mimics several aspects of lung O_2 toxicity observed clinically, and rats exposed to 85% O_2 for 5-7 days acquire tolerance to the otherwise lethal effects of exposure to 100%

O_2 (Crapo 1975; Crapo et al. 1980; Evelson and Gonzalez-Flecha 2000; Hayatdavoudi et al. 1981; Johnson et al. 1998). This tolerance is not observed in other rodents, but a similar tolerance occurs in humans (Capellier et al. 1999; Crapo and Tierney 1974). Elucidating the underlying mechanisms of this tolerance could lead to the identification of therapeutic targets for protection from lung O_2 toxicity and oxidant-induced acute lung injury.

Previous studies have demonstrated hyperoxia-induced changes in the activities of redox enzymes, predominantly in lung tissue homogenates, and have suggested that redox enzymes, among other factors, play a role in rat tolerance to 100% O_2 following exposure to 85% O_2 (Crapo et al. 1980; Crapo and Tierney 1974; Ho, Dey, and Crapo 1996; Kimball et al. 1976). However, the results of these *in vitro* studies do not necessarily predict hyperoxia-induced changes in the activities of redox enzymes in an intact lung (Audi et al. 2005; Audi et al. Oxygen dependency of monoamine oxidase activity in the intact lung 2001). This is because potential changes in key aspects of the enzyme environment in an intact lung (e.g., competing redox enzymes, availability of electron donors, tissue perfusion) that may influence redox enzyme kinetics are not preserved *in vitro* (Audi et al. 2005). Thus, a hyperoxia-induced change in the activity of a redox enzyme measured in lung tissue homogenate may not be representative of the change in its activity in the intact lung (Audi et al. 2005; Audi et al. Oxygen dependency of monoamine oxidase activity in the intact lung 2001). Studies evaluating redox enzyme kinetics in the intact lung have lagged behind the tremendous advances of *in vitro* cell biology, in part, because of the functional complexity of the intact lung.

Indicator dilution methods have been important research tools for evaluating metabolic functions within an organ of interest (Audi et al. 2003; Audi et al. Oxygen dependency of monoamine oxidase activity in the intact lung 2001; Bassingthwaighte 1998; Dawson 2003; Schwab and Goresky 1996; Zierhut et al. 2007). These methods involve the bolus injection or finite pulse infusion of two or more indicators into the organ's arterial inlet, followed by the measurement of concentrations of these indicators in the venous effluent as a function of time. The injected indicators usually include a vascular indicator plus a test indicator that is a substrate or ligand for the organ's metabolic function(s) of interest. The interactions of the test indicator with these metabolic function(s) on passage though the organ, result in characteristic differences between the vascular and test indicator venous effluent concentration versus time curves (Audi et al. 1994; Audi et al. 1995).

The information content in the data resulting from indicator dilution methods can be complex, because, in addition to the targeted tissue metabolic processes, several other factors can influence the amount of indicator that is removed and/or modified on passage through the organ (Audi et al. 1998). These include organ perfusion kinematics (e.g., capillary mean transit time, distribution of capillary transit times), lung tissue accessible to the test indicator from the vascular space and reactions taking place in the blood (e.g., plasma-protein binding). Thus, for a given test indicator, a change in measured indicator dilution data could result from change in the activities of metabolic processes with which the test indicator interacts and/or changes in one or more of the above factors. Therefore, proper interpretation of indicator dilution data requires information about these factors, including organ perfusion kinematics, and the use of mathematical models that account

for all these factors (Audi et al. 2003; Audi et al. Oxygen dependency of monoamine oxidase activity in the intact lung 2001; Bassingthwaighte 1998; Dawson 2003; Schwab and Goresky 1996; Zierhut et al. 2007).

Audi et al. have used indicator dilution methods and mathematical modeling to evaluate the activities of redox enzymes in the isolated perfused rat lungs (Audi et al. 2003; Audi et al. 2005; Audi et al. Pulmonary reduction of an intravascular redox polymer 2001; Audi et al. Oxygen dependency of monoamine oxidase activity in the intact lung 2001; Audi et al. 2000; Dawson et al. 2000). For instance, Audi et al. have demonstrated that the redox active quinone test indicator duroquinone (DQ) is reduced to durohydroquinone (DQH_2) on passage through the pulmonary circulation in the isolated perfused rat lung, wherein DQH_2 appears in the venous effluent. Inhibitor studies revealed that NAD(P)H: quinone oxidoreductase 1 (NQO1) is the dominant reductase involved in the reduction of DQ to DQH_2, and that the capacity of the lung to reduce DQ to DQH_2 is a measure of NQO1 activity in the intact lung (Audi et al. 2003). NQO1 is predominantly a cytoplasmic anti-oxidant enzyme that is induced in response to oxidative stress (Audi et al. 2003; Cadenas 1995; Merker et al. 2004). Rat exposure to 85% O_2 for 21 days, as a model of pulmonary oxidative stress, increased the capacity of the lung to reduce DQ to DQH_2, as well as lung tissue NQO1 activity and protein levels (Audi et al. 2005).

Recently, Audi et al. demonstrated the capacity of the rat lung to reduce the redox active quinone test indicator 2,3-dimethoxy-5-methyl-6-[3-methyl-2-butenyl]-1,4-benzoquinone (coenzyme Q_1; CoQ_1) to its hydroquinone form (CoQ_1H_2), and to oxidize CoQ_1H_2 to CoQ_1 on passage through the pulmonary circulation (Audi et al. 2008). CoQ_1

is a homolog of ubiquinone which is the endogenous quinone electron carrier in the

mitochondrial electron transport chain located at the inner mitochondrial membrane (Di

Virgilio and Azzone 1982; Fato et al. 1996; Merker et al. 2007; Rich and Harper 1990).

Moreover, ubiquinone participates in other redox functions, as an anti- and pro-oxidant

substance (Chan et al. 2002). Inhibitor studies revealed that mitochondrial complex I and

NQO1 are the dominant sites of CoQ_1 reduction on passage through the lung, and that

mitochondrial complex III is the dominant site of CoQ_1H_2 oxidation (Audi et al. 2008).

Both complexes I and III are important sources of reactive oxygen species (ROS) (Audi

et al. 2008). Audi et al. demonstrated that rat exposure to 85% O_2 for 48 hrs decreased the

overall capacity of the lung to reduce CoQ_1 to CoQ_1H_2, predominantly due to ~47%

decrease in the capacity of mitochondrial complex I mediated CoQ_1 reduction. This

hyperoxia-induced decrease in lung complex I activity is potentially important to lung O_2

toxicity since mitochondrial complex I is a major source of ROS (Brueckl et al. 2006;

Turrens 2003).

Preliminary indicator dilution studies in Dr. Audi's laboratory have demonstrated

that rat exposure to 85% O_2 for 7 days, which confers tolerance to 100% O_2, alters the

capacity of the rat lung to metabolize various redox active test indicators, including

CoQ_1, DQ, DQH_2 and CoQ_1H_2, on their passage through the pulmonary circulation.

Quantitative interpretation of the resulting indicator dilution data in terms of the effect of

hyperoxia on the lung activities of redox enzymes, including NQO1 and mitochondrial

complexes I and III, requires information about the effect of hyperoxia on the other

factors that could affect the redox metabolism of DQ and CoQ_1 on passage through the

pulmonary circulation, including lung capillary mean transit time ($\bar{t}_c$) and the distribution

of capillary transit times ($h_c(t)$) (Audi et al. 1998). This is important, especially, since the

pulmonary capillary endothelium is a primary target of O_2 toxicity, and since vascular

remodeling involving loss of capillary volume and endothelial surface area has been

reported for this hyperoxia model (Crapo et al. 1980). To the best of our knowledge, there

is no known information about the effect of rat exposure to 85% O_2 for 7 days on $h_c(t)$.

Thus, the objective of this study was to evaluate the effect of rat exposure to hyperoxia

(85% O_2 for 7 days) on the lung capillary mean transit time and the distribution of

capillary transit times. The 7-day exposure period was chosen since there are several

existing studies that have investigated the effect of this hyperoxia model on lung cellular

composition, capillary volume and capillary endothelial surface area (Crapo et al. 1980).

1.2   Methods for measuring lung capillary volume, mean transit time and/or capillary transit time distribution

Several methods have been used previously to estimate rat lung capillary volume,

mean transit time and/or transit time distribution (Ahuja 2007; Audi et al. 1994; Clough et

al. 1994; Clough et al. 1998; Clough, Linehan, and Dawson 1997; Presson et al. 1997;

Randell, Mercer, and Young 1990; Sjostrom and Crapo 1983; Wagner et al. 1982;

Wagner et al. 1986). What follows is a brief description of each of these methods, and

their inherent strengths and limitations.

Morphometric methods have been used to evaluate the rat lung capillary volume

and endothelial surface area (Crapo et al. 1980; Randell, Mercer, and Young 1990;

Sjostrom and Crapo 1983). Generally speaking, morphometric methods involve fixing the

lung tissue by injecting a fixative into the pulmonary artery, following which the lung is

sectioned. Stereology is then used to estimate morphometric parameters such as capillary volume and capillary surface area. Using a morphometric approach, Crapo et al. demonstrated that, compared to room air rats, rats exposed to hyperoxia (85% O_2 for 7 days) showed a ~53% decrease in the pulmonary capillary lumen volume, and in turn the capillary mean transit time (Crapo et al. 1980). However, morphometric methods can be tedious and can lead to over-estimation of the lung capillary volume due to the effect of tissue fixation on the lung capillary transmural pressure (Audi et al. 1994; Audi et al. 1995). Moreover, these methods cannot be used to measure the distribution of lung capillary transit times.

Glenny et al. developed a method for measuring capillary flow distribution using fluorescent microspheres (Glenny, Bernard, and Robertson 2000). The method involves the injection of fluorescent microspheres into the lung. The lung is then cut into pieces and microsphere deposition is measured in each piece. Assuming that microsphere deposition is proportional to capillary blood flow distribution, an estimate of capillary blood flow distribution can be obtained. Based on certain assumptions about the relationship between capillary flow distribution and transit time distribution, the capillary transit time distribution can then be estimated (Audi et al. 1998; King, Raymond, and Bassingthwaighte 1996). Glenny et al. used fluorescent microspheres in rats to determine the coefficient of variation of lung microsphere deposition, which is a measure of the heterogeneity of capillary flow distribution, at varying sampling volumes. They found that the coefficient of variation increased with decreasing sampling volumes down to the acinar level (Glenny, Bernard, and Robertson 2000). Thus, their study indicated the presence of capillary perfusion heterogeneity in the rat lung and also showed that it

increased continuously as progressively smaller lung regions were examined. Although this method provides spatial information about capillary blood flow distribution, it is destructive and the results are dependent on sampling volume. Moreover, it does not provide an estimate of the lung capillary mean transit time.

Wagner et al. introduced a method for measuring capillary mean transit time and transit time distribution on the lung surface using fluorescence microscopy (Wagner et al. 1982; Wagner et al. 1986). The method involves the injection of a fluorescent dye into the lobar artery and observing its passage through the pleural capillaries using *in vivo* microscopy. Presson et al. used a similar approach to measure the capillary mean transit time and the transit time distribution in rat lung subpleural capillaries by direct video-microscopic recording of a fluorescent dye on its passage through the rat subpleural microcirculation (Presson et al. 1997). They selected a microscopic field that contained a single arteriole and a single venule of equal or smaller diameter for their measurements. This method relies on the assumption that the subpleural capillary network adequately represents the entire pulmonary capillary network. However, there are morphometric differences between subpleural and intrapulmonary capillary beds (Guntheroth, Luchtel, and Kawabori 1982; Miller 1947), which suggest that their estimates may not be representative of whole lung $h_c(t)$, although Presson et al. suggested that these differences might not be significant for the rat lung (Presson et al. 1997).

Clough et al. developed an X-ray microfocal angiography method for estimating $h_c(t)$ in an isolated perfused dog lung lobe (Clough, Linehan, and Dawson 1997). The method involves imaging the passage of a bolus of radiopaque contrast through the lung vasculature using microfocal X-ray angiography. Time-absorbance curves at the inlet to

the lobar artery, outlet of the lobar vein, and microvasculature are acquired from the images by positioning regions-of-interest (ROIs) over the acquired images. The overall dispersion of the bolus within the lung lobe is then estimated from the differences in the first and second moments, namely the mean transit time and variance, respectively, of the inlet and the outlet time-absorbance curves. The lobar capillary transit time distribution is estimated by model-based deconvolution of the lobar artery inlet absorbance curve and the microvascular ROI absorbance curve. Ahuja (Ahuja 2007) used this method to measure the capillary transit time distribution in lung lobes from normal and hyperoxic (85% O_2 for 14 days) rats. The results of her study showed that exposure of rats to 85% O_2 for 14 days decreased lobar capillary volume by ~37% with no significant effect on the heterogeneity of lobar capillary transit time distribution (Ahuja 2007). One of the problems encountered by Ahuja was that she could not measure the capillary transit time distribution for the entire lung due to the confounding effects of other pre-lobar vessels in the background. Moreover, owing to the relatively short lengths of the rat lobar artery and lobar vein, use of the microfocal angiography approach in rat lung lobes was found to be sensitive to the placement of the lobar arterial and venous cannulae (Ahuja 2007).

Goresky proposed an indicator dilution method called the 'linear superposition method' for estimating the capillary volume and transit time distribution (Goresky 1963). The method involves the arterial bolus injection of a vascular indicator and a flow-limited indicator, and the simultaneous measurement of their concentrations in the venous effluent as a function of time. Vascular indicators are confined to the vascular bed on passage through the organ. A flow-limited indicator is a compound that rapidly equilibrates between blood and tissue on passage through an organ's capillary or

microvascular region (Audi et al. 1994; Audi et al. 1995; Goresky 1963). The capillary

wall presents no barrier to its diffusion and flow is the only factor that limits the

exchange of a flow-limited indicator between blood and tissue. Under the assumption that

no dispersion occurs outside the capillary bed, Goresky showed that the flow-limited

indicator venous effluent concentration versus time outflow curve ($C_F(t)$) is a scaled

version of the vascular indicator outflow curve ($C_R(t)$). The scaling process requires two

parameters λ and $\bar{t}_n$, where λ is the ratio of the flow-limited indicator extravascular

volume to the capillary volume, and $\bar{t}_n$ is the transit time through the organ's conducting

vessels (arteries and veins), which is assumed to be the same for the vascular and flow-

limited indicators. The scaling process involves the following sequence of steps: a)

shifting the time axis of $C_F(t)$ backward by $\bar{t}_n$, b) scaling the concentration and shifted

time axes of $C_F(t)$ by $(1+\lambda)$ and $1/(1+\lambda)$, respectively, c) shifting the time axis of the

scaled $C_F(t)$ forward by $\bar{t}_n$ (Audi 1998). The linear superposition method involves

finding the values of λ and $\bar{t}_n$ that minimize the sum of squared differences between

$C_R(t)$ and the scaled $C_F(t)$ (Audi et al. 1995). Audi et al. utilized this approach to estimate

the capillary transit time distribution in the isolated perfused rabbit lung with either [3]H-

alfentanil or [14]C- diazepam as the flow-limited indicator (Audi et al. 1995).

Audi et al. developed an indicator dilution (MID) method for estimating the capillary

transit time distribution in an intact lung (Audi et al. 1994; Audi et al. 1995; Audi 1998),

which relaxes the Goresky assumption of no vascular dispersion outside the capillary

bed. The method is based on the following algebraic equations that relate the mean transit

time (first moment; $\bar{t}$), the variance (second central moment; σ^2), and the skewness (third

central moment; m^3) of the concentration versus time outflow curves of a vascular

indicator ($C_R(t)$) and a flow-limited indicator ($C_F(t)$), following their arterial bolus injection, to those of the capillary transit time distribution $h_c(t)$.

$$\sigma_F^2 - \sigma_R^2 = \left(\left(1 + \frac{\bar{t}_e}{\bar{t}_c}\right)^2 - 1\right)\sigma_c^2 \qquad (1.1a)$$

$$m_F^3 - m_R^3 = \left(\left(1 + \frac{\bar{t}_e}{\bar{t}_c}\right)^3 - 1\right)m_c^3 \qquad (1.1b)$$

where the subscripts R, F and c refer to $C_R(t)$, $C_F(t)$, and $h_c(t)$ respectively. The extravascular mean residence time for the flow-limited indicator is given by

$$\bar{t}_e = \bar{t}_F - \bar{t}_R$$

Figure 1.1 (panel a.) shows the concentration versus time outflow curves of the vascular indicator fluorescein isothiocyanate dextran (FITC-dex) and the lipophilic amines test indicators ^{3}H-alfentanil and ^{14}C-diazepam following their arterial bolus injection into the pulmonary artery of an isolated perfused rat lung. These test indicators behave as flow-limited indicators on passage through lungs from rats exposed to room air (panel a) (Audi et al. 2003; Audi et al. 1995). For each of these outflow curves, C(t), the shape of the curve can be described by its mean transit time (first moment; $\bar{t}$), variance (second central moment; σ^2), and skewness (third central moment; m^3), which can be determined using the following equations:

$$\bar{t} = \frac{\int_0^\infty t\, C(t)\, dt}{\int_0^\infty C(t)\, dt} \qquad (1.2a)$$

$$\sigma^2 = \frac{\int_0^\infty (t - \bar{t})^2\, C(t)\, dt}{\int_0^\infty C(t)\, dt} \tag{1.2b}$$

$$m^3 = \frac{\int_0^\infty (t - \bar{t})^3\, C(t)\, dt}{\int_0^\infty C(t)\, dt} \tag{1.2c}$$

The mean transit time is a measure of the average time the indicator spends in the organ, the variance is a measure of the distribution of C(t) about the mean transit time, and the skewness is a measure of the asymmetry of the distribution of C(t) around the mean. Estimation of the first three moments of $h_c(t)$ using Equations (1.1a-b) requires knowledge of the first three moments of the concentration versus time outflow curves of a vascular indicator $C_R(t)$ and at least two flow-limited indicators $C_F(t)$ with sufficiently different $\bar{t}_e$ on passage through the lung (Audi et al. 1994; Audi et al. 1995).

Audi et al. applied this MID method first in isolated perfused dog lung lobes using ^{14}C-diazepam as the flow-limited indicator. Since diazepam participates in rapidly equilibrating interactions with perfusate albumin, the tissue-to-plasma partition coefficient of ^{14}C-diazepam, and hence its apparent $\bar{t}_e$, could be adjusted by altering the perfusate albumin concentration. Thus, by making two injections of ^{14}C-diazepam, each at a different perfusate albumin concentration, data equivalent to making one injection with two different flow-limited indicators having different $\bar{t}_e$ values were obtained (Audi et al. 1994). Subsequently, Audi et al. used the method in isolated rabbit lungs, with lipophilic amines, ^{3}H-alfentanil and [14]C- diazepam, as the two flow-limited indicators with different $\bar{t}_e$ values (Audi et al. 2003; Audi et al. 1995).
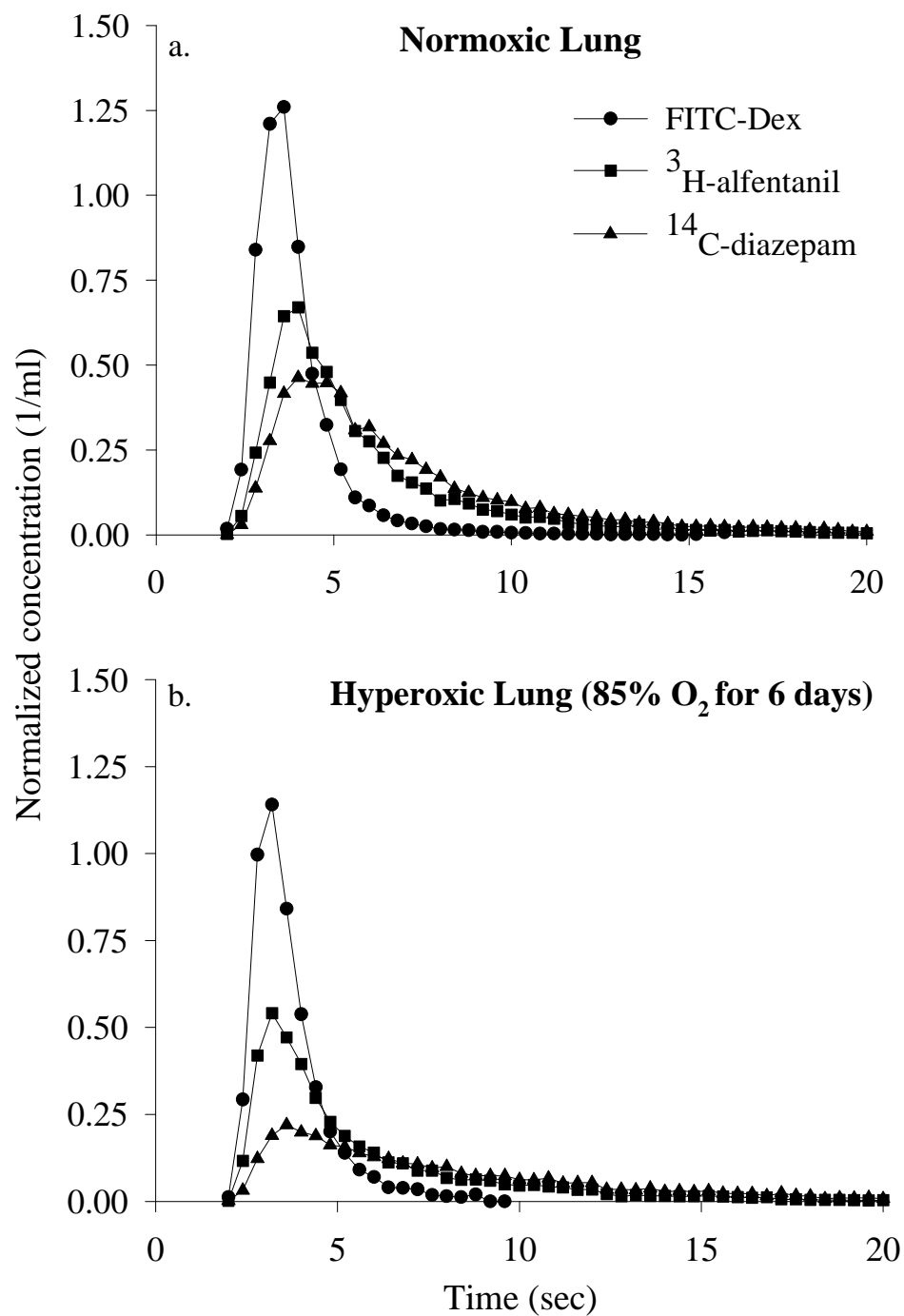
Figure 1.1: Venous effluent FITC-dex, ^{3}H-alfentanil and ^{14}C-diazepam concentration versus time curves in a normoxic lung (panel a.) and a hyperoxic lung (85% O_2 for 6 days, panel b.). The recoveries for ^{3}H-alfentanil and ^{14}C-diazepam in the venous effluent were ~100% for the normoxic lung, and ~85% and ~65% for the hyperoxic lung, respectively.

Using ^{3}H-alfentanil and ^{14}C- diazepam, Audi et al. estimated the pulmonary capillary transit time distribution in normoxic isolated perfused rat lungs (Audi et al. 2003). They estimated a vascular volume of ~0.85 ± 0.06 (SE) ml, a capillary volume of ~0.47 ± 0.02 ml and a capillary relative dispersion (RD_c) of ~0.91 ± 0.03, where RD_c is a non-dimensional measure of the heterogeneity of $h_c(t)$. The use of this approach for evaluating the effect of rat exposure to hyperoxia (85% O_2 for 7 days) on lung capillary mean transit time and $h_c(t)$ requires that alfentanil and diazepam exhibit flow-limited behavior on passage through the pulmonary circulation of lungs from rats exposed to this hyperoxia model. Upon subsequent examination, results (unpublished) revealed that neither alfentanil nor diazepam exhibit flow-limited behavior in lungs from rats exposed to 85% O_2 for 6 to 8 days. Figure 1.1 shows the concentration versus time outflow curves of ^{3}H-alfentanil, ^{14}C- diazepam, and the vascular indicator FITC-dex following the bolus injection of these indicators into the arterial inlets of an isolated perfused lung from a normoxic rat (panel a.), and from a rat exposed to 85% O_2 for 6 days (panel b.). For the normoxic lung, the recoveries of the injected alfentanil and diazepam in the venous effluent were not significantly different from 100%. However, for the hyperoxic lung, only 65% of the injected diazepam and 85% of the injected alfentanil were recovered in the venous effluent. This suggests that both alfentanil and diazepam participate in slowly dissociating interactions on passage through the hyperoxic lung and hence do not behave as flow-limited indicators (Audi et al. 2002).

Recently, Audi et al. demonstrated that the reduced form (CoQ_1H_2) of the quinone compound coenzyme Q_1 behaves as a flow-limited indicator on passage through the isolated perfused lungs of rats exposed to room air or to 85% O_2 for 48 hrs (Audi et al.

2008). This suggests using CoQ_1H_2 as one of the two flow-limited indicators for evaluating $h_c(t)$ in hyperoxic rat lungs using the method represented by Equations (1.1a-b). As an alternative to searching for a second flow-limited indicator with an extravascular mean residence time ($\bar{t}_e$) different from that of CoQ_1H_2, one could exploit the fact that CoQ_1H_2 binds to perfusate albumin in a rapidly equilibrating manner (Audi et al. 2008). Audi et al. derived the following relationship between the perfusate albumin concentration and the extravascular mean residence time of a flow-limited indicator that rapidly interacts with perfusate protein on passage through the lung.

$$\bar{t}_e = \frac{M\,Q_t}{F\left(1 + \frac{[P]}{K}\right)} \qquad (1.3)$$

where, M is the tissue-to-plasma partition coefficient of the flow-limited indicator, K is the indicator-plasma protein binding equilibrium dissociation constant, F is the perfusate flow, Q_t is the extravascular tissue volume accessible by the flow-limited indicator, and [P] is the perfusate albumin concentration (Audi et al. 1994; Audi et al. 1995).

Equation 1.3 suggests that $\bar{t}_e$ is inversely proportional to perfusate albumin concentration [P]. Thus, the value of $\bar{t}_e$ for CoQ_1H_2 on passage through the lung could be manipulated by altering the perfusate albumin concentration. Hence, bolus injections of CoQ_1H_2 at different perfusate albumin concentrations would provide data equivalent to bolus injections of multiple flow-limited indicators with different $\bar{t}_e$ values. Hence, the specific aims of this study are to:

1) evaluate the effect of manipulating perfusate albumin concentration on CoQ_1H_2 extravascular mean residence time ($\bar{t}_e$) during its passage through the isolated perfused rat lung, and to select the albumin concentrations that result in CoQ_1H_2 curves with sufficiently different $\bar{t}_e$ values,

2) utilize the MID method developed by Audi et al., with CoQ_1H_2 at different perfusate albumin concentrations as the flow-limited indicators, to evaluate the effect of rat exposure to hyperoxia (85% O_2 for 7 days) on rat lung capillary mean transit time and transit time distribution.

2. EXPERIMENTAL METHODS

2.1   Materials

Coenzyme Q_1 (CoQ_1) and other chemicals, unless noted, were purchased from Sigma (St. Louis, MO). CoQ_1H_2 was prepared by reduction of CoQ_1 with potassium borohydride (KBH_4) as previously described (Audi et al. 2005). Bovine serum albumin (BSA) was purchased from Serologicals Inc. (Gaithersburg, MD).

2.2   Oxygen exposure

For normoxic lung studies, Sprague-Dawley rats (~300 g; Charles River) were exposed to room air with free access to food and water. For the hyperoxic lung studies, age matched rats were housed in a Plexiglas chamber (13W x 23L x 12H inches) (Figure 2.1) maintained at ~85% O_2, balance N_2, for 7 days with free access to food and water as previously described (Audi et al. 2005). The total gas flow was ~3.5 liters/min and the chamber CO_2 was maintained at < 0.5 %. The temperature within the chamber was maintained at ~21°C using a custom built cooling system. The chamber was opened every other day for ~15 min to clean the cage, weigh the animals, and replace food, water, and CO_2 absorbent. The protocol was approved by the Institutional Animal Care and Use Committees of the Veterans Affairs Medical Center and Marquette University (Milwaukee, WI). A total of 9 normoxic rats and 5 hyperoxic rats were studied.

Figure 2.1: Sprague-Dawley rats in the Plexiglas exposure chamber. Flow meters were used to regulate the inflow of air and O_2 and to maintain the chamber O_2 at 85%.

2.3   Isolated perfused lung preparation

The isolated perfused rat lung preparation has been previously described (Audi et al. 2005; Audi et al. 2008). Each rat was anesthetized with pentobarbital sodium (40 mg/kg body wt. i.p.). The trachea was clamped, the chest was opened, and heparin (0.7 IU/g body wt.) was injected into the right ventricle. The pulmonary artery and the trachea were cannulated, and the pulmonary venous outflow was accessed via a cannula in the left atrium. The lung was removed from the chest and attached to a ventilation-perfusion system. The control perfusate contained in mM 4.7 KCl, 2.51 $CaCl_2$, 1.19 $MgSO_4$, 2.5 KH_2PO_4, 118 NaCl, 25 $NaHCO_3$, 5.5 glucose, and 5% BSA (Audi et al. 2003; Audi et al. 2005; Audi et al. 2008). The single pass perfusion system was primed with the control

perfusate maintained at 37°C and equilibrated with 15% O_2, 6% CO_2, balance N_2,

resulting in perfusate PO_2, PCO_2 and pH of ~105 Torr, 40 Torr, and 7.4, respectively. An

injection loop was included in the arterial line to allow the introduction of a ~0.1 ml

bolus into the arterial inflow without altering the flow or perfusion pressure (Audi et al.

2003; Audi et al. 2005; Audi et al. 2008). Initially, control perfusate was pumped through

the lung until the lung was evenly blanched and the venous effluent was clear of blood, as

determined by visual inspection. The lung was ventilated (40 breaths/min) at end-

inspiratory and end-expiratory pressures of 6 and 3 mmHg, respectively, with the above

gas mixture. The pulmonary arterial pressure was referenced to atmospheric pressure at

the level of the left atrium and monitored continuously during the course of the

experiments. The venous outflow was referenced to atmospheric pressure. At the end of

each experiment, the lung was weighed, and then dried (60°C) to a constant weight for

the determination of lung dry weight.

2.4   Experimental protocols

Table 2.1 shows a schematic diagram of the experimental protocol described

below. An index of perfused capillary surface area was estimated as previously described

(Audi et al. 2005; Audi et al. 2008). Briefly, a 150 μM 20-second pulse infusion of the

ACE substrate N-[3-(2-Furyl) acryloyl]-Phe-Gly-Gly (FAPGG) was introduced into the

lung with the flow set at 30 ml/min. Two venous effluent samples (~1.0 ml each) were

collected between 15 and 20 seconds after the start of the infusion (Audi et al. 2005; Audi

et al. 2008). The permeability-surface area product (PS, ml/min) for FAPGG, which is a

measure of the rate of ACE mediated FAPGG hydrolysis, was determined from the

FAPGG concentrations measured in the venous effluent samples as previously described

(Audi et al. 2005; Audi et al. 2008):

$$PS = -F \ln\left(1 - E\right) \tag{2.1}$$

where E = steady state extraction ratio $= 1 - \dfrac{[FAPGG]_o}{[FAPGG]_i}$;

$[FAPGG]_i$ is the infused arterial FAPGG concentration; $[FAPGG]_o$ is the steady state

venous effluent FAPGG concentration calculated as the average [FAPGG] in the

collected venous effluent samples, and F is the perfusate flow. The PS product is

considered here as an index of perfused capillary surface area (Audi et al. 2005; Audi et

al. 2008).

Table 2.1: Schematic diagram of the experimental protocol

Treatment		Potassium Cyanide (2 mM)			
Flow	30 ml/min	10 ml/min			30 ml/min
Pefusate	5% BSA	5%BSA	3% BSA	10% BSA	5% BSA
Indicator dilution experiment	FAPGG pulse infusion	FITC-dex and CoQ_1H_2 bolus injections	CoQ_1H_2 bolus injection	CoQ_1H_2 bolus injection	FAPGG pulse infusion

Time

For each lung, the FAPGG pulse infusion was carried out at the beginning and at

the end of the CoQ_1H_2 and FITC-dex bolus injection protocol described below to

evaluate the stability of the lung by this measure over the time course of the experiment.

For both FAPGG pulse infusions the lung was perfused with control perfusate.

15% O_2, 6% CO_2

Masterflex Roller Pump (Flow-rate: 10ml/min)

Pulmonary Artery

Pulmonary Vein

Bolus of FITC - dex or CoQ_1H_2

Rat lung

Perfusate with 3%, 5% or 10% BSA concentration

FITC - dex or CoQ_1H_2 venous effluent samples collected using a fraction collector
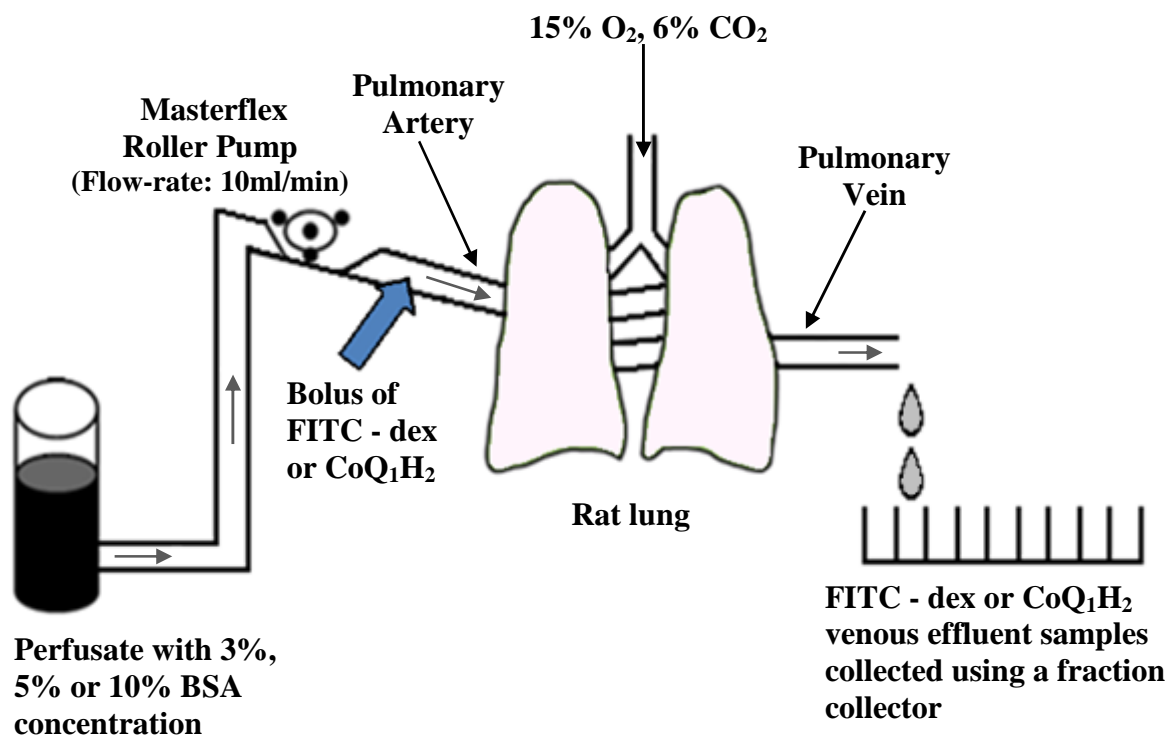
Figure 2.2: Schematic diagram of the rat lung ventilation-perfusion system. Arrows indicate the direction of perfusate flow.

After the first FAPGG pulse infusion, each lung was perfused with control

perfusate containing 2 mM potassium cyanide (KCN) for 5 min at 10 ml/min to inhibit

mitochondrial complex III, which is the main site of CoQ_1H_2 oxidation on passage

through the rat lung (Audi et al. 2008). The respirator was then stopped at end expiration

and a 0.1 ml bolus of control perfusate containing 2 mM KCN and either 35 μM FITC-

dex (vascular indicator) or 1200 μM CoQ_1H_2 (flow-limited indicator) was injected into

the pulmonary arterial inflow tubing. Simultaneous to each bolus injection, the venous

effluent was diverted into a modified Gilson Escargot fraction collector for continuous

collection (Audi et al. 2003; Audi et al. 2005; Audi et al. 2008). For the FITC-dex bolus

injection, sixty samples (0.15 ml each) were collected at a sampling interval of 0.9 sec at

a flow of 10 ml/min. For the CoQ_1H_2 injection, sixty samples (0.3 ml each) were

collected at a sampling interval of 1.8 sec at a flow of 10 ml/min. Two reasons for the

difference in sampling intervals (volumes) of FITC-dex and CoQ_1H_2 are: 1) the

minimum CoQ_1H_2 sampling volume (and hence the sampling time) is limited by the

sensitivity of the assay used to measure the concentration of CoQ_1H_2 in the venous

effluent samples; 2) the rate of change in the concentration of FITC-dex in the venous

effluent is greater than that for CoQ_1H_2, which necessitates a smaller sampling interval

for FITC-dex, especially around the peak of its concentration versus time outflow curve.

To determine the influence of perfusate albumin binding of CoQ_1H_2 on its

pulmonary disposition, we examined the influence of perfusate BSA concentration on the

concentration versus time outflow curve of CoQ_1H_2 following its arterial bolus injection.

After the first two bolus injections with perfusate containing 5% BSA (control perfusate),

the perfusate reservoir was refilled with an appropriate volume of fresh perfusate

containing 3% BSA and 2 mM KCN. This was followed by another 0.1 ml bolus

injection of 3% BSA perfusate containing KCN and CoQ_1H_2, and a sampling of the

venous effluent as described above. Following this, another CoQ_1H_2 bolus injection was

carried out after adjusting the reservoir perfusate BSA concentration to 10% in the

presence of KCN. The choice of 3% and 10% BSA concentrations were based on

Equation 1.3, which predicts a ~50% increase and decrease in the $\bar{t}_e$ of CoQ_1H_2

compared to the control perfusate (5% BSA) at perfusate BSA's of 3% and 10%, respectively.

At the end of the bolus injection and pulse infusion protocols, the lung was removed from the perfusion system, the arterial and venous cannulae were connected, and the reservoir was refilled with control perfusate. This was followed by an FITC-dex (35 μM) bolus injection at a pefusate flow of 10 ml/min. Thirty samples (0.15 ml each) were collected at a sampling interval of 0.9 sec. From this data, we determined the tubing transit time of the perfusion system and the bolus dispersion outside the lung.

2.5   Determination of CoQ_1H_2 and FITC-dex in venous effluent samples

The concentrations of CoQ_1H_2 in the venous effluent samples were determined as previously described (Audi et al. 2003; Audi et al. 2005; Audi et al. 2008). The venous effluent samples were first centrifuged (1 min at 5,600 g). For each sample, 100 μl of supernatant was then added to a centrifuge tube containing 10 μl potassium ferricyanide (12.1 mM in deionized H_2O) to oxidize any CoQ_1H_2 to CoQ_1. Cold absolute ethanol (~0.6 ml) was added and the tube was mixed on a vortex mixer followed by centrifugation at 9,300 g for 5 min at 4°C. A perfusate sample that had passed through the lungs, but contained no CoQ_1H_2, was treated in the same manner to be used as the blank for absorbance measurements. Sample concentration of CoQ_1, in μM, was calculated from the absorbance (Abs) value (Beckman DU 7400 spectrophotometer) at 275 nm of the fully oxidized supernatant in the tube using a molar extinction coefficient of 14.30 mM^{-1} cm^{-1} as follows:

$$[CoQ_1] = \frac{Abs}{0.0143} \qquad (2.1)$$

where $[CoQ_1]$ is the concentration of CoQ_1 in the samples, which is also the sample

concentration of CoQ_1H_2 prior to the addition of potassium ferricyanide to oxidize

CoQ_1H_2 to CoQ_1. Thus, for a given venous sample, $[CoQ_1H_2]$ is given by Equation (2.2):

$$[CoQ_1H_2] = \frac{Abs}{0.0143} \qquad (2.2)$$

The concentration of FITC-dex in each venous effluent sample was determined

from the sample absorbance at 495 nm using a molar extinction coefficient of 93.5

mM^{-1} cm^{-1} (Audi et al. 2003; Audi et al. 2005; Audi et al. 2008).

The respective calculated recoveries for FITC-dex and CoQ_1H_2 in the venous

effluent samples following their arterial bolus injections were 93.25 ± 5.8 (SE) % and

101.27 ± 1.1 % for normoxic lungs, and 106.22 ± 5.2 % and 109.37 ± 3.4 % for

hyperoxic lungs, respectively, none of which were significantly different from 100%.

2.6 Statistical analysis

Statistical comparisons were carried out using an unpaired *t*-test or ANOVA,

followed by Tukey's test, with $P < 0.05$ as the criterion for statistical significance.

3. EXPERIMENTAL RESULTS

3.1   Physiological parameters

Figure 3.1 shows the normalized body weights of rats exposed to 85% O_2 at different time points during the 7-day exposure period. For the first 48 hrs of hyperoxic exposure, rats gained weight. Between days 2 and 6, rat body weights decreased steadily. However, by day 7, the rats stopped losing body weight. Over the 7-day exposure period, rats lost ~10 % of their pre-exposure body weights (Figure 3.1).
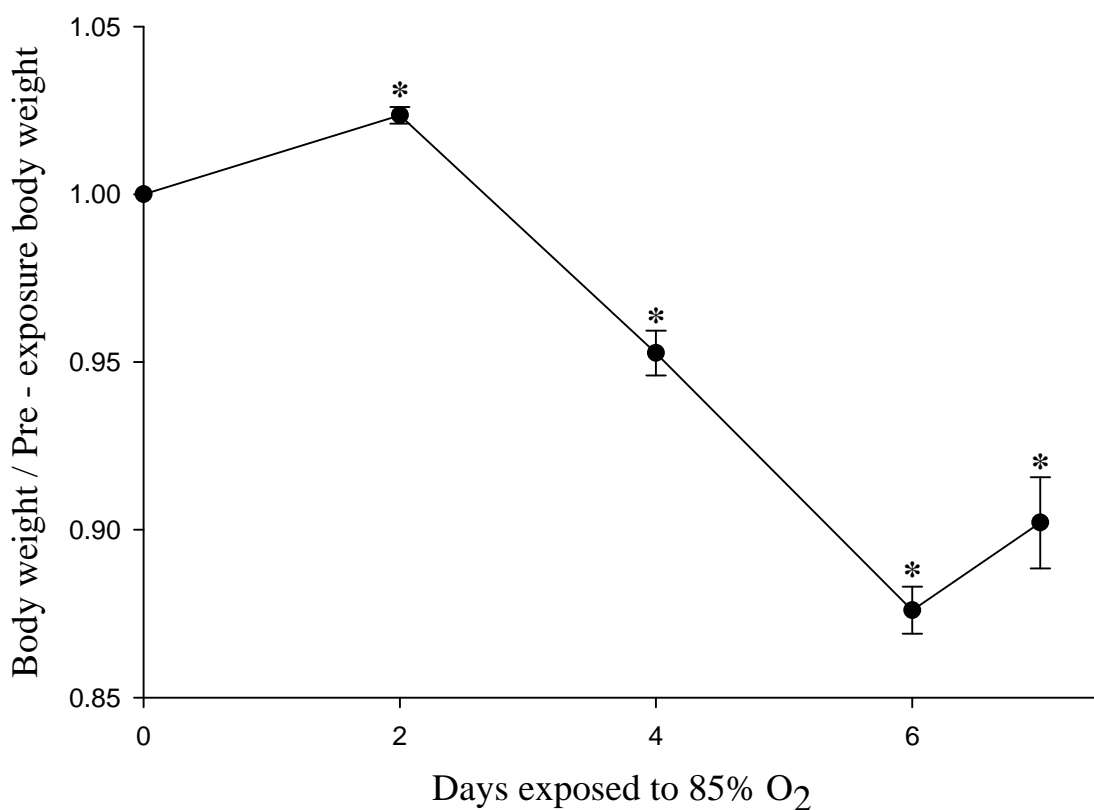
Figure 3.1: Rat body weights normalized to pre-exposure body weights at different time points during the 7-day exposure period. Values are mean $\pm$ SE (n = 5). * indicates values that are significantly different from the body weight on day 0 (t-test; $p < 0.05$).

Rat exposure to hyperoxia significantly increased lung wet and dry weights, with no significant effect on lung wet/dry weight ratios or lung perfusion pressure at 10 ml/min or 30 ml/min as compared to normoxic lungs (Table 3.1). The lung wet weights of hyperoxic rats measured in the present study are consistent with those reported by Crapo et al. (2.29 ± 0.44 (SD) g for ~290 g rats) for the same hyperoxia model (Crapo et al. 1980). The lack of a significant difference in wet/dry weight ratio between normoxic and hyperoxic lungs suggests that the increase in wet weights of hyperoxic lungs was due to infiltration of cells rather than due to edema (Crapo et al. 1980). Changes in perfusate BSA % had no significant effect on lung perfusion pressure for normoxic and hyperoxic lungs (data not shown).

Exposure to hyperoxia increased the circulatory blood hematocrit (Table 3.1). This increase is consistent with that observed by Crapo et al. after 7 days of exposure to 85% O_2, which could be in part due to dehydration (Crapo et al. 1980).

Table 3.1: Body weights, lung wet weights, dry weights and wet/dry weight ratios, circulatory blood hematocrit (Hct) and lung perfusion pressures (P_a) for normoxic and hyperoxic rats.

	Body wt (g)	Wet wt (g)	Dry wt (g)	Wet/dry wt	Hct (%)	P_a (Torr) 10ml/min	P_a (Torr) 30 ml/min
Normoxic lungs	292 ± 9	1.20 ± 0.07	0.21 ± 0.01	5.76 ± 0.16	42.9 ± 0.7	5.0 ± 0.3	9.9 ± 0.5
Hyperoxic lungs	283 ± 5	2.40 ± 0.21*	0.41 ± 0.04*	5.87 ± 0.09	49.42 ± 0.7*	5.6 ± 0.3	10.0 ± 0.5

n = 9 and 5 for normoxic and hyperoxic (85% O_2 for 7 days) rats, respectively. Values are mean ± SE. * indicates values that are significantly different between normoxic and hyperoxic lungs (t-test; $p < 0.05$).

3.2 **Lung ACE activity and perfused capillary surface area**

The permeability-surface area product (PS, ml/min) for FAPGG, which is a measure of the rate of ACE mediated FAPGG hydrolysis, is considered here as an index of perfused capillary surface area (Audi et al. 2005; Audi et al. 2008). Exposure to hyperoxia decreased PS (ml/min) on average by ~58 % (Table 3.2). The PS values obtained from FAPGG pulse infusions carried out at the beginning or at the end of a given experimental protocol were not significantly different, indicating that perfusion and/or multiple bolus injections of CoQ_1H_2 and FITC-dex did not have significant irreversible effects on lung capillary endothelial surface area and/or angiotensin converting enzyme (ACE) activity. Therefore, by these measures, the lungs were stable over the time course of the experimental bolus injection protocol.

Table 3.2: Angiotensin converting enzyme (ACE) activity in normoxic and hyperoxic lungs

	PS (ml/min) (Start)	PS (ml/min) (End)
Normoxic lungs	17.5 ± 1.0	15.7 ± 1.2
Hyperoxic lungs	$7.7 \pm 0.5^*$	$6.4 \pm 0.2^*$

PS (permeability surface area product), a measure of the rate of ACE mediated FAPGG hydrolysis and an index of perfused capillary surface area, evaluated at the start and the end of the bolus injection experiments for normoxic (n = 9) and hyperoxic (n = 5) rat lungs. Values are mean ± SE. * indicates values that are significantly different between normoxic and hyperoxic lungs (t-test; $p < 0.05$).

3.3 FITC-dex and CoQ_1H_2 bolus injections

Figure 3.2 shows an example of venous effluent concentration versus time curves of FITC-dex and CoQ_1H_2, obtained after bolus injections of FITC-dex and CoQ_1H_2 into the arterial inlet of a normoxic lung (panel a.) and a hyperoxic lung (panel b.) perfused with perfusate containing three different BSA concentrations. The FITC-dex concentration versus time curves indicate what the effluent CoQ_1H_2 curves would have looked like, had the CoQ_1H_2 not interacted with the lung tissue as it passed through the pulmonary vessels (the effect of convection alone). For the normoxic lung (panel a.), the CoQ_1H_2 curves are shifted to the right (indicating longer transit times on account of CoQ_1H_2 accessing lung tissue volume) and more dispersed (lower peaks and longer tails) relative to the FITC-dex curve, consistent with the flow-limited behavior of CoQ_1H_2 in the lung tissue (Audi et al. 2003; Audi et al. 2005). Moreover, the CoQ_1H_2 curves show a progressive increase in the transit time (first moment) of CoQ_1H_2 as perfusate BSA concentration decreased. For the hyperoxic lung (panel b.), the FITC-dex curve has a higher peak than that for the normoxic lung, consistent with a decrease in lung vascular volume. The CoQ_1H_2 curves are also more dispersed than the FITC-dex curve, and the transit time of CoQ_1H_2 is inversely proportional to perfusate BSA concentration. However, for the hyperoxic lung, the peaks of the CoQ_1H_2 curves are less shifted to the right of the peak of the FITC-dex curve as compared to the normoxic lung.

Figure 3.2: Venous effluent FITC-dex and CoQ_1H_2 normalized concentration (as a fraction of the injected amount per milliliter of effluent perfusate) vs. time data following the bolus injection of the indicators upstream from the pulmonary artery of a normoxic (panel a.) and a hyperoxic (panel b.) lung perfused at three different perfusate % BSA concentrations. Lungs were treated with potassium cyanide (KCN) prior to bolus injection to inhibit complex III mediated CoQ_1H_2 oxidation on its passage through the lung. For the FITC-dex curve, the perfusate BSA concentration was 5%.

4. DATA ANALYSIS

4.1 Estimation of the moments of FITC-dex and CoQ$_1$H$_2$ concentration versus time outflow curves

For a given concentration versus time outflow curve, C(t), following the bolus

injection of FITC-dex or CoQ$_1$H$_2$, the mean transit time ($\bar{t}$), the variance (σ^2), and the

third central moment (skewness; m^3) can be calculated using Equation (4.1).

$$\bar{t} = \frac{\int_0^\infty tC(t)\,dt}{\int_0^\infty C(t)\,dt} \; ; \sigma^2 = \frac{\int_0^\infty \left(t - \bar{t}\right)^2 C(t)\,dt}{\int_0^\infty C(t)\,dt} ; \; m^3 = \frac{\int_0^\infty \left(t - \bar{t}\right)^3 C(t)\,dt}{\int_0^\infty C(t)\,dt} \qquad (4.1)$$

To minimize the effect of noise in the tails of the FITC-dex and CoQ$_1$H$_2$

concentration versus time outflow curves (Figure 3.2) on the estimated values of $\bar{t}$, σ^2

and m^3, we utilize a model-based approach to estimate these moments as an alternative to

Equation (4.1) (Audi et al. 2003; Audi et al. 1998; Audi et al. 1995). Thus, for a given

C(t), $\bar{t}$, σ^2 and m^3 were obtained by fitting a shifted random walk function (SRWF) to

C(t). SRWF is a probability density function whose functional form is defined by

Equation (4.2)

$$\text{SRWF(t)} = \begin{cases} 0 & \text{, for } t \leq t_s \\\\ \dfrac{\sqrt{\dfrac{\theta\phi}{4\pi(t - t_s)}}}{\theta} \exp\left(\dfrac{-\phi\left(1 - \dfrac{t - t_s}{\theta}\right)^2}{4\dfrac{t - t_s}{\theta}}\right) & \text{, for } t > t_s \end{cases} \qquad (4.2)$$

SRWF(t) has the property that, $\int_0^\infty SRWF(t) = 1$. The SRWF(t) parameters θ, ϕ and t_s are related to $\bar{t}$, σ^2 and m^3 by the following equations (Audi et al. 1996):

$$\bar{t} = \theta\left(1 + \frac{2}{\phi}\right) + t_s \tag{4.3a}$$

$$\sigma^2 = \frac{2\phi + 8}{(\phi + 2)^2}(t - t_s)^2 \tag{4.3b}$$

$$m^3 = \frac{12\phi + 64}{\phi^3}\theta^3 \tag{4.3c}$$

The fitting procedure consists of finding the values of θ, ϕ and t_s for which Equation (4.2), scaled by the inverse of the flow (F), best fits C(t) in the least-squares sense. The nonlinear parameter optimization procedure was carried out using the MATLAB 7.0.1 subroutine '*lsqcurvefit*', which solves a non-linear curve fitting problem in the least-squares sense (The MathWorks, Inc.) using the Levenberg-Marquardt algorithm. Figure 4.1 shows examples of the SRWF fits to FITC-dex and CoQ_1H_2 concentration versus time outflow curves from a normoxic and a hyperoxic lung. For both normoxic and hyperoxic lungs, the Coefficient of Variation (CV), which is a normalized measure of the goodness of fit of the SRWF to the concentration versus time outflow curves, was ~12.2 % for FITC-dex and ~12.6 % for CoQ_1H_2.

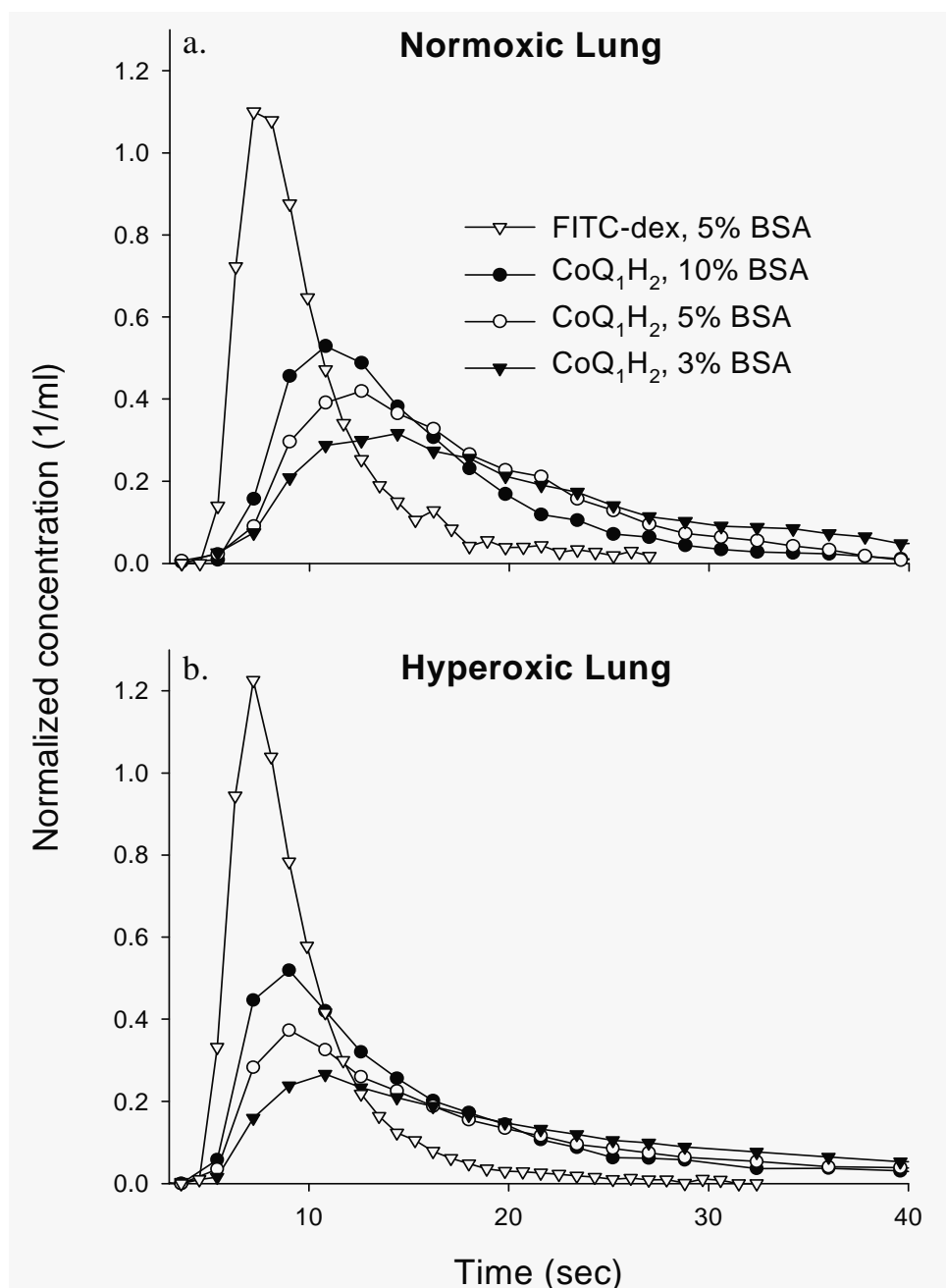**Figure 4.1:** Venous effluent FITC-dex and CoQ_1H_2 normalized concentration (as a fraction of the injected amount per milliliter of effluent perfusate) vs. time data following the bolus injection of the indicators upstream from the pulmonary artery of a normoxic (panel a.) and a hyperoxic (panel b.) lung perfused with perfusate containing different % BSA concentrations. Solid lines are SRWF fits.

4.2   Evaluation of the assumption of rapidly equilibrating interactions of CoQ_1H_2 with plasma albumin (BSA) and with lung tissue

The CoQ_1H_2 apparent extravascular mean residence time ($\bar{t}_e$) at a given perfusate BSA concentration was determined by subtracting the mean transit time of the FITC-dex outflow curve ($C_R(t)$) from that of the CoQ_1H_2 outflow curve ($C_F(t)$) measured with the lung connected to the ventilation-perfusion system (Figure 3.2), i.e.,

$$\bar{t}_e = \bar{t}_F - \bar{t}_R \tag{4.4}$$

where $\bar{t}_R$ and $\bar{t}_F$ are the mean transit times of $C_R(t)$ and $C_F(t)$, respectively, and their values were determined as described above.

Audi et al. considered the relationship between the apparent extravascular mean residence time ($\bar{t}_e$) and perfusate albumin concentration [BSA] for a flow-limited indicator for the case in which 1) the equilibration of the free form of the indicator between perfusate and tissue and 2) the association-dissociation of the indicator with plasma protein and with lung tissue occur rapidly in comparison to the capillary mean transit time (Audi et al. 1994; Audi et al. 1995). They showed that

$$\frac{1}{\bar{t}_e F} = \frac{1}{MQ_t} + \left(\frac{1}{MQ_t}\right)\frac{[BSA]}{K} \tag{4.5}$$

where, M is the tissue-to-plasma partition coefficient of the flow-limited indicator, Q_t is the tissue volume accessible to the flow-limited indicator from the vascular region, K is the indicator-BSA binding equilibrium dissociation constant, F is the perfusate flow, and $Q_e = \bar{t}_e F$ is the apparent extravascular volume of the flow-limited indicator (Audi et al. 1994; Audi et al. 1995).

With the value of K^{-1} for CoQ_1H_2 set to 3.8 per % [BSA] as previously estimated

(Audi et al. 2008), Equation (4.5) is a one-parameter linear model with slope and

intercept = $1/MQ_t$. Equation (4.5) was fit separately to the mean values of $\dfrac{1}{\bar{t}_e F}$ versus

$\dfrac{[BSA]}{K}$ for normoxic and hyperoxic lungs (Figure 4.2).
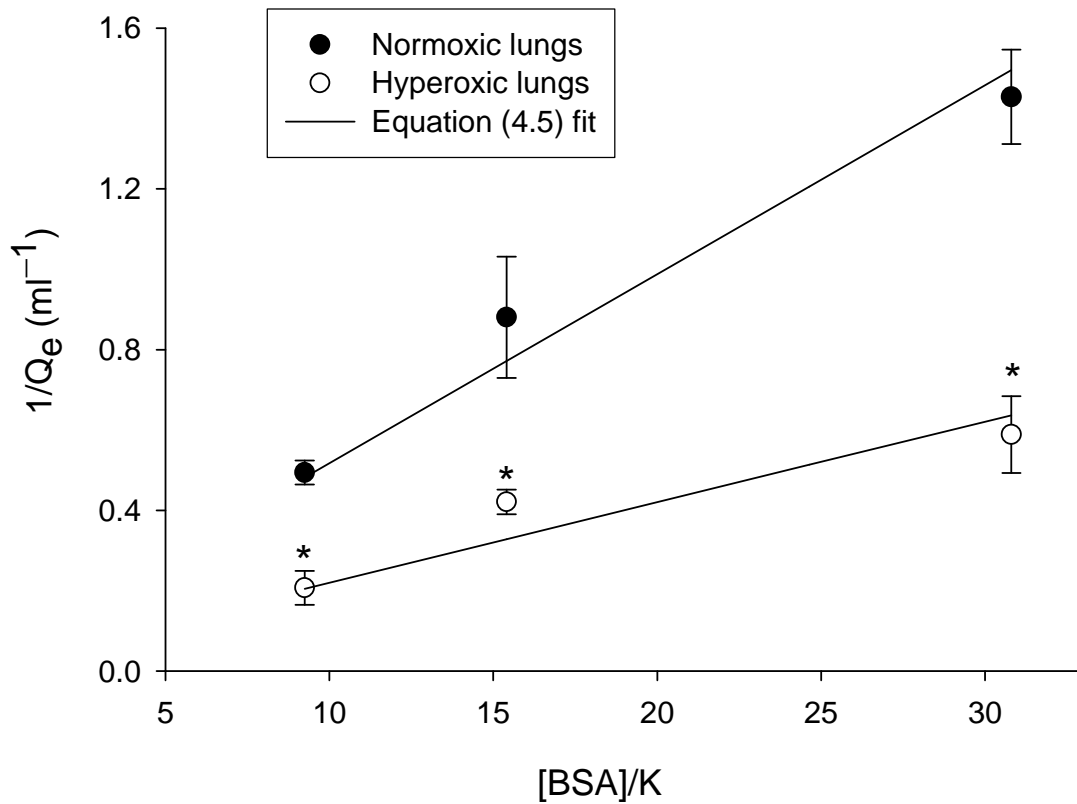
Figure 4.2: Symbols are data from normoxic (n = 6) and hyperoxic (n = 5) rat lung experiments plotted according to Equation (4.5). K^{-1} was 3.8/ % BSA (Audi et al. 2008). The extravascular volume Q_e is the product of the extravascular mean residence time ($\bar{t}_e$) and flow (F). [BSA] and K represent the concentration of BSA (%) present in the perfusate, and the indicator-BSA binding equilibrium dissociation constant, respectively. Solid lines indicate Equation (4.5) fit to data, resulting in a slope = intercept = 4.7×10^{-2} ml^{-1} for normoxic lungs ($r^2 = 0.98$) and 2.0×10^{-2} ml^{-1} for hyperoxic lungs ($r^2 = 0.85$). * indicates values that are significantly different between normoxic and hyperoxic lungs (t-test; $p < 0.05$).

The ability of Equation (4.5) to fit the data in Figure 4.2 reasonably well (r^2 = 0.98 and 0.85 for normoxic and hyperoxic lungs, respectively) supports the rapidly equilibrating assumption of CoQ_1H_2 with perfusate BSA and tissue in normoxic and hyperoxic lungs (Audi 1993; Audi et al. 1994; Audi et al. 1995).

Rat exposure to hyperoxia increased the apparent extravascular mean residence time ($\bar{t}_e$) for CoQ_1H_2 at all three perfusate BSA concentrations studied (Figure 4.2). For instance, the value of $\bar{t}_e$ at a perfusate BSA of 5% for hyperoxic lungs was ~73% larger than that for normoxic lungs. This increase in $\bar{t}_e$ values could be due to hyperoxia-induced increase in lung wet weight accessible to CoQ_1H_2 from the vascular region (Table 3.1) and/or hyperoxia-induced increase in CoQ_1H_2 tissue-to-perfusate partition coefficient (M).

4.3   Effect of exposure to hyperoxia on lung vascular volume and vascular transit time distribution

The lung vascular mean transit time ($\bar{t}_v$) and variance of the vascular transit time distribution (σ_v^2) were obtained by finding the difference between the mean transit times ($\bar{t}$) and variances (σ^2) of the FITC-dex curves measured with the lung in place ($C_R(t)$), and with the lung removed (tubing; $C_{tub}(t)$) from the perfusion system (Figure 4.3), i.e.,

$$\bar{t}_v = \bar{t}_R - \bar{t}_{tub} \tag{4.6}$$

$$\sigma_v^2 = \sigma_R^2 - \sigma_{tub}^2 \tag{4.7}$$

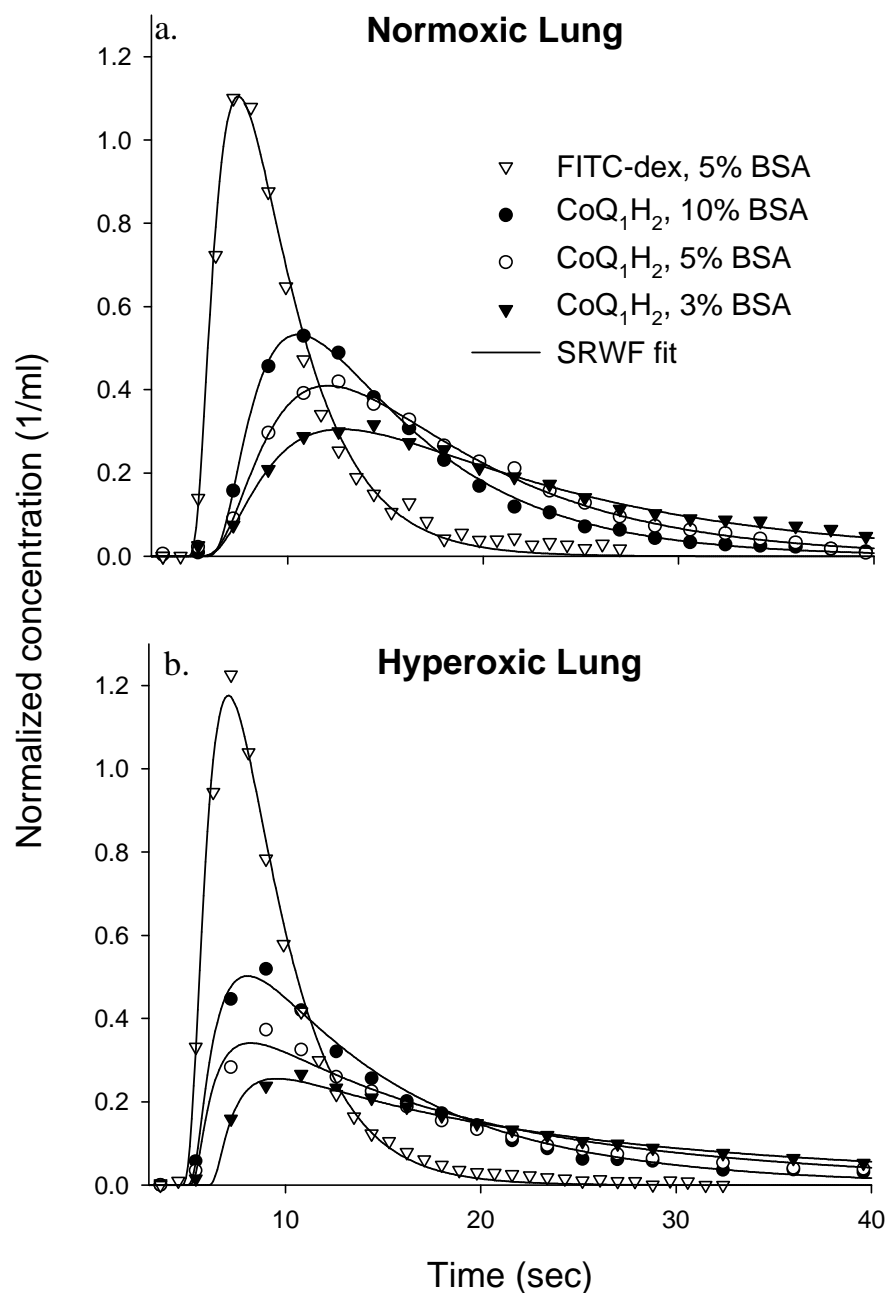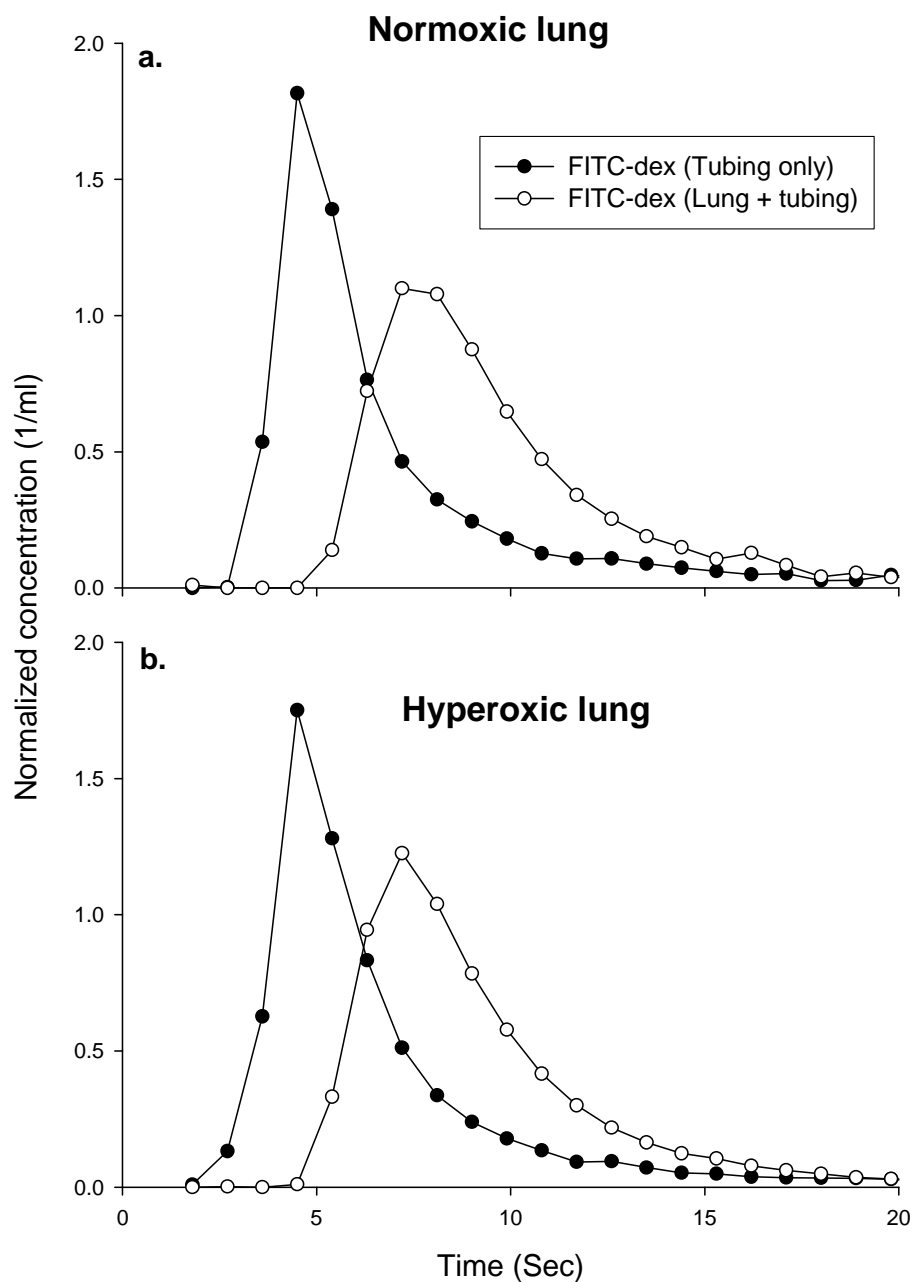**Figure 4.3:** Venous effluent FITC-dex normalized concentration (as a fraction of injected amount per milliliter of effluent perfusate) vs. time data collected with and without the lung connected to the ventilation perfusion system for a normoxic (panel a.) and a hyperoxic (panel b.) lung.

The lung vascular volume (Q_v) was determined as the product of $\bar{t}_v$ and the perfusate flow (F).

$$Q_v = \bar{t}_v \cdot F \tag{4.8}$$

The relative dispersion (RD_v), which is a dimensionless measure of the heterogeneity of lung vascular transit time distribution, was calculated using Equation (4.9)

$$RD_v = \sqrt{\sigma_v^2} / \bar{t}_v \tag{4.9}$$

Table 4.1 shows that rat exposure to hyperoxia decreased $\bar{t}_v$ and Q_v by ~21%, with no significant effect on σ_v^2 or RD_v.

Table 4.1: Lung vascular mean transit times, variances, relative dispersions, volumes, and apparent CoQ_1H_2 extravascular volumes

	$\bar{t}_v$ (sec)	σ_v^2 (sec^2)	RD_v	Q_v (ml)	Q_e (ml)
Normoxic lungs	4.18 ± 0.26	4.05 ± 0.63	0.47 ± 0.02	0.70 ± 0.04	1.41 ± 0.11
Hyperoxic lungs	$3.29 \pm 0.17^*$	2.82 ± 0.52	0.50 ± 0.04	$0.55 \pm 0.03^*$	$2.44 \pm 0.22^*$

$\bar{t}_v$, σ_v^2, RD_v and Q_v are the lung vascular mean transit time, variance of vascular transit times, the relative dispersion of the vascular transit time distribution, and the vascular volume, respectively. Q_e is the apparent extravascular volume for CoQ_1H_2 for lungs perfused with control perfusate (5% BSA). n = 9 (normoxic) and 5 (hyperoxic) for all parameters. Values are mean $\pm$ SE. * indicates values that are significantly different between normoxic and hyperoxic lungs (t-test; $p < 0.05$).

4.4   Effect of rat exposure to hyperoxia on lung capillary mean transit time, volume and transit time distribution

Method A

The approach developed by Audi et al. (referred to as method A in (Audi et al. 1994) for estimating the moments of $h_c(t)$ is based on Equations (4.10a-b), which relate the moments ($\bar{t}_c$, σ_c^2 and m_c^3) of $h_c(t)$ to those of the concentration versus time outflow curves of a vascular indicator ($C_R(t)$) and a flow-limited indicator ($C_F(t)$).

$$\sigma_e^2 = \sigma_F^2 - \sigma_R^2 = \left[\left(1 + \frac{\bar{t}_e}{\bar{t}_c}\right)^2 - 1\right]\sigma_c^2 \qquad (4.10a)$$

$$m_e^3 = m_F^3 - m_R^3 = \left[\left(1 + \frac{\bar{t}_e}{\bar{t}_c}\right)^3 - 1\right]m_c^3 \qquad (4.10b)$$

where $\bar{t}_e = \bar{t}_F - \bar{t}_R$ and the subscripts c, R and F represent $h_c(t)$, $C_R(t)$ and $C_F(t)$, respectively. Equations (4.10a-b) with three unknowns, namely, $\bar{t}_c$, σ_c^2 and m_c^3, represent an underdetermined system. Hence, estimating the values of these unknowns using Equations (4.10a-b) requires at least two flow-limited indicators having different $\bar{t}_e$ values (Audi et al. 1994; Audi et al. 1995). For the present study, the outflow curves of CoQ_1H_2 at the three different perfusate BSA concentrations (Figure 4.1) represent three flow-limited indicators with different $\bar{t}_e$ values (Figure 4.2). For the purpose of parameter estimation, Equations (4.10 a-b) were re-written as follows (Audi et al. 1994):

$$\sigma_{ei}^2 = \sigma_{Fi}^2 - \sigma_R^2 = \left[\left(1 + \frac{\bar{t}_{ei}}{\bar{t}_c}\right)^2 - 1\right]\sigma_c^2 \qquad (4.11a)$$

$$m_{ei}^3 = m_{Fi}^3 - m_R^3 = \left[\left(1 + \frac{\bar{t}_{ei}}{\bar{t}_c}\right)^3 - 1\right] m_c^3 \qquad (4.11b)$$

where $i = 1,2,..., j$, and j represents the number of flow-limited indicators ($j = 3$ for the data in Figure 4.1), each with a different extravascular mean residence time $\bar{t}_{ei}$. The moments of $h_c(t)$ are then estimated using nonlinear least squares approximation using the above equations in the following forms (Audi et al. 1994; Audi et al. 1995):

$$F\left(\bar{t}_{ei}, \sigma_{ei}^2, \bar{t}_c, \sigma_c^2\right) = \left\{\sqrt{\left[\left(1 + \frac{\bar{t}_{ei}}{\bar{t}_c}\right)^2 - 1\right]\sigma_c^2 - \sqrt{\sigma_{ei}^2}}\right\}\bigg/\sqrt{\sigma_{ei}^2} \qquad (4.12a)$$

$$G\left(\bar{t}_{ei}, m_{ei}^3, \bar{t}_c, m_c^3\right) = \left\{\sqrt[3]{\left[\left(1 + \frac{\bar{t}_{ei}}{\bar{t}_c}\right)^3 - 1\right]m_c^3 - \sqrt[3]{m_{ei}^3}}\right\}\bigg/\sqrt[3]{m_{ei}^3} \qquad (4.12b)$$

The optimization routine finds the values of $\bar{t}_c$, σ_c^2 and m_c^3, that minimize the term (4.13).

$$\sum_{i=1}^{j} F\left(\bar{t}_{ei}, \sigma_{ei}^2, \bar{t}_c, \sigma_c^2\right)^2 + G\left(\bar{t}_{ei}, m_{ei}^3, \bar{t}_c, m_c^3\right)^2 \qquad (4.13)$$

The lower bounds on $\bar{t}_c$, σ_c^2 and m_c^3 were set at zero. The vascular skewness m_R^3 was set as the upper bound on m_c^3. The upper bounds on σ_c^2 and $\bar{t}_c$ were $\sigma_{c_{max}}^2$ (Equation 4.14a) and $\bar{t}_{c_{max}}$, (Equation 4.14b), respectively.

$$\sigma^2_{c_{max}} = \frac{\sigma^2_{ei}}{\left(1 + \frac{m^3_{ei}}{m^3_R}\right)^{2/3} - 1} \tag{4.14a}$$

$$\bar{t}_{c_{max}} = \frac{\bar{t}_{ei}}{\sqrt{1 + \frac{\sigma^2_{ei}}{\sigma^2_{c_{max}}} - 1}} \tag{4.14b}$$

The values of $\bar{t}_c$, σ^2_c and m^3_c, estimated from the moments of the FITC-dex and CoQ$_1$H$_2$ outflow curves using Method A are given in Table 4.2, which shows that exposure to hyperoxia increased RD$_c$ by ~31%, with no significant effect on $\bar{t}_c$, σ^2_c or m^3_c. The estimated values of $\bar{t}_c$ ranged between 1.14 sec and 2.49 sec for normoxic lungs, and 0.74 sec and 1.8 sec for hyperoxic lungs. The estimated values of σ^2_c ranged between 0.97 sec^2 and 3.38 sec^2 for normoxic lungs, and 0.66 sec^2 and 3.75 sec^2 for hyperoxic lungs. This wide range in the estimated values of $\bar{t}_c$ and σ^2_c for the normoxic and hyperoxic lungs is due to the high correlation between $\bar{t}_c$ and σ^2_c in Equation 4.13. This correlation was revealed by fixing $\bar{t}_c$ at 50 % above or below the estimated value of $\bar{t}_c$ for one normoxic lung and then estimating the values of σ^2_c and m^3_c using Equation 4.13. This reduced the number of unknown parameters in Equation 4.13 from three to two. Table 4.3 shows that the sum of squared errors (SSE) between Equation 4.13 fit and the data was not significantly affected (F-test) by fixing the value of $\bar{t}_c$ over a wide range (Motulsky and Ransnas 1987). The SSE is the sum of the squares of the deviation of every point in the fit from its corresponding point in the original data.

Table 4.2: Lung capillary mean transit times, variances, skewnesses, relative dispersions and volumes estimated using Method A

	$\bar{t}_c$ (sec)	σ_c^2 (sec^2)	m_c^3 (sec^3)	RD_c
Normoxic lungs (n = 9)	1.55 ± 0.18	1.72 ± 0.31	4.44 ± 1.22	0.84 ± 0.02
Hyperoxic lungs (n = 5)	1.33 ± 0.22	2.35 ± 0.65	9.36 ± 3.27	1.10 ± 0.02 [*]

$\bar{t}_c$, σ_c^2, m_c^3, and RD_c are the pulmonary capillary mean transit time, variance of capillary transit times, skewness of capillary transit times, and relative dispersion of the capillary transit time distribution, respectively. Values were estimated using Equations (4.12a-b). Values are mean $\pm$ SE. * indicates values that are significantly different between normoxic (n = 9) and hyperoxic (n = 5) lungs (t-test; p < 0.05).

Table 4.3: Effect of fixing the value of $\bar{t}_c$ on the estimated values of σ_c^2, m_c^3, and the goodness of Equation 4.13 with two parameters to data

	$\bar{t}_c$ (sec)	σ_c^2 (sec^2)	m_c^3 (sec^3)	RD_c	SSE
Estimated value of $\bar{t}_c$	1.14	0.97	1.95	0.87	0.0074
$\bar{t}_c$ fixed at 50% of its estimated value	0.57	0.27	0.29	0.92	0.0088
$\bar{t}_c$ fixed at 150% of its estimated value	1.71	1.98	5.53	0.82	0.0084

$\bar{t}_c$, σ_c^2, m_c^3, RD_c and SSE are the pulmonary capillary mean transit time, variance of capillary transit times, skewness of capillary transit times, relative dispersion of the capillary transit time distribution and the sum of squared errors between Equation 4.13 fit and data. Values were estimated using Equations (4.12a-b).

In order to better understand the basis for the high correlation between parameters estimated using Method A, we carried out a sensitivity analysis. Sensitivity functions are used to evaluate the sensitivity of a given set of data to a given parameter and the ability of a given set of data to separately identify multiple parameters (Bassingthwaighte and Chaloupka 1984). Two parameters are said be dependent or highly correlated if their sensitivity functions are identical or algebraically related. Based on Equation (4.10 a-b), the sensitivities of σ_e^2 to $\bar{t}_c$ and σ_c^2 are given by Equations (4.15 a-b).

$$\frac{\partial \sigma_e^2}{\partial t_c} = 2\,\sigma_c^2 \left(1 + \frac{t_e}{t_c}\right)\left(-\frac{t_e}{t_c^2}\right) \tag{4.15a}$$

$$\frac{\partial \sigma_e^2}{\partial \sigma_c^2} = \left[\left(1 + \frac{t_e}{t_c}\right)^2 - 1\right] \tag{4.15b}$$

Previously, Audi et al. (Audi et al. 2003) estimated values of 2.8 sec and 0.9 for the capillary mean transit time and relative dispersion of the capillary transit time distribution in the isolated perfused normoxic rat lung. Assuming these values for $\bar{t}_c$ and RD_c, Equations (4.15a-b) were evaluated for $\bar{t}_e$ values ranging from 1 to 100 seconds. The ratio of the sensitivity functions of σ_e^2 to $\bar{t}_c$ and σ_c^2 (Equations (4.15 a-b)) was then plotted as a function of $\bar{t}_e/\bar{t}_c$ (Figure 4.4). For $\bar{t}_e/\bar{t}_c > 3$, the ratio of the sensitivity functions for $\bar{t}_c$ and σ_c^2 appears to be virtually independent of the value of $\bar{t}_e$. Hence, for $\bar{t}_e/\bar{t}_c > 3$ the values of σ_e^2 at different $\bar{t}_e$ values are not sufficient to separately identify $\bar{t}_c$ and σ_c^2. For the data exemplified in Figure 4.1, the values of $\bar{t}_e$ ranged between 5 and 12 sec for normoxic lungs and 11 and 35 sec for hyperoxic lungs. For a $\bar{t}_c$ value of 2.5 sec, the $\bar{t}_e/\bar{t}_c$ ratio at perfusate BSA concentrations of 10, 5 and 3% are ~2, 4 and 6 for

normoxic lungs and 4, 6 and 12 for hyperoxic lungs, respectively. Even for normoxic lungs, the range of $\bar{t}_e$ values is close to that where the correlation between $\bar{t}_c$ and σ_c^2 would be expected to be relatively high. Thus, to be able to use method A to evaluate the effect of hyperoxia on lung capillary volume and transit time distribution, one would need to identify at least two flow-limited indicators with $\bar{t}_e$ values that are not only different, but are also small enough relative to $\bar{t}_c$ to break the correlation between $\bar{t}_c$ and σ_c^2.
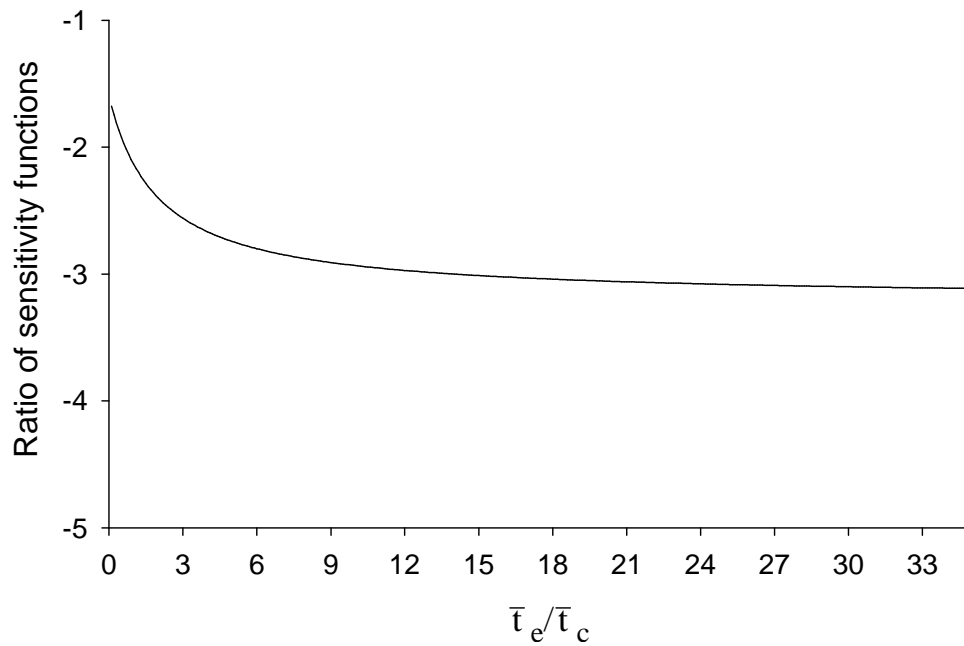
Figure 4.4: Ratio of the sensitivity functions (Equations (4.15 a-b)) of σ_e^2 to $\bar{t}_c$ and σ_c^2 plotted as a function of $\bar{t}_e/\bar{t}_c$. The values of $\bar{t}_c$ and RD_c used were 2.8 sec and 0.9, respectively.

Method B1

Previous studies have demonstrated that > 90% of the variance of the lung

vascular transit time distribution in the dog lung lobe, rabbit lung and rat lung was due to

the capillary bed (Ahuja 2007; Audi et al. 2003; Audi et al. 1994; Audi et al. 1995;

Clough et al. 1998). Thus, one approach for breaking the correlation between $\overline{t}_c$ and σ_c^2

in Equation (4.10a) would be to set the value of σ_c^2 to σ_v^2, which is the variance of the

lung vascular transit time distribution (Table 4.1). This approach is referred to as **Method**

B1 in (Audi et al. 1994). Under this assumption, algebraic manipulation of Equation

(4.10a) leads to the following relationship between $\overline{t}_c$ and the extravascular moments of a

flow-limited indicator outflow curve ($C_F(t)$) (Audi et al. 1994; Audi et al. 1995).

$$\overline{t}_c = \frac{\overline{t}_e}{\sqrt{1 + \dfrac{\sigma_e^2}{\sigma_v^2}} - 1} \tag{4.16}$$

where $\sigma_e^2 = \sigma_F^2 - \sigma_R^2$. Thus, the moments of one flow-limited indicator would be

sufficient to determine $\overline{t}_c$ using Equation (4.16).

Model simulations (see *Discussion* section) revealed that if 10% of σ_v^2 occurred

outside the capillary bed (i.e., in the conducting vessels), the estimated value of $\overline{t}_c$ using

Equation (4.16) would be overestimated by ~7%. Thus, we used Equation (4.16) to

estimate $\overline{t}_c$ under the assumption that σ_c^2 is equal to σ_v^2.

Table 4.4 shows the values of $\overline{t}_c$ estimated from the moments of CoQ_1H_2 outflow

curves measured at the three different perfusate BSA concentrations. For both normoxic

and hyperoxic lungs, perfusate BSA concentration had no effect on the estimated values

of $\bar{t}_c$ using Equation (4.16). However, for all three perfusate BSA concentrations studied, the estimated values of $\bar{t}_c$ for hyperoxic lungs were ~42% lower as compared to those for normoxic lungs (Table 4.4). Furthermore, the estimated values of the capillary relative dispersion RD_c were ~40% higher for hyperoxic lungs as compared to normoxic lungs. The capillary volume as a fraction of the total lung volume was ~60% and ~40% in normoxic and hyperoxic lungs, respectively.

Table 4.4: Estimated values of the capillary mean transit time and relative dispersion as a function of perfusate BSA concentration for normoxic and hyperoxic lungs

	3% BSA		5% BSA		10% BSA	
	$\bar{t}_c$ (sec)	RD_c	$\bar{t}_c$ (sec)	RD_c	$\bar{t}_c$ (sec)	RD_c
Normoxic	2.45 ± 0.37	0.82 ± 0.05	2.44 ± 0.33	0.78 ± 0.03	2.59 ± 0.29	0.77 ± 0.02
Hyperoxic	1.45 ± 0.15*	1.14 ± 0.01*	1.44 ± 0.16*	1.15 ± 0.02*	1.41 ± 0.15*	1.17 ± 0.03*

$\bar{t}_c$ and RD_c are the pulmonary capillary mean transit time and relative dispersion of the capillary transit time distribution, respectively. Values are mean ± SE, n = 6 and 5 for normoxic and hyperoxic lungs, respectively. * indicates values that are significantly different between normoxic and hyperoxic lungs (t-test; p < 0.05).

One way to evaluate the assumption that the variance of the total vascular transit time distribution (σ_v^2) is due to the capillary bed, would be to rearrange Equation (4.16). This results in Equation (4.17), which suggests the following relationship between $\bar{t}_e$ and σ_e^2 with one unknown parameter, namely $\bar{t}_c$.

$$\sigma_e^2 = \frac{\sigma_v^2}{\bar{t}_c^2}\bar{t}_e^2 + 2\frac{\sigma_v^2}{\bar{t}_c}\bar{t}_e \tag{4.17}$$

The ability of Equation (4.17) to fit the σ_e^2 versus $\bar{t}_e$ data (Figure 4.5) for the

normoxic and hyperoxic bolus injection data exemplified in Figure 4.1 is consistent with

the above assumption. Table 4.5 shows that the values of $\bar{t}_c$ estimated using Equation

(4.17) for normoxic and hyperoxic lungs are virtually the same as those in Table 4.4

estimated using Equation (4.16). So $\bar{t}_c$ could be estimated using either Equation (4.16) or

Equation (4.17).

Table 4.5: Values of capillary mean transit time, variance, relative dispersion and
volume in normoxic and hyperoxic lungs estimated using Method B1

	$\bar{t}_c$ (sec)	σ_c^2 (sec^2)	RD$_c$	Q$_c$ (ml)	Q$_c$ /Q$_v$
Normoxic lungs	2.45 ± 0.26	4.05 ± 0.63	0.82 ± 0.03	0.41 ± 0.04	0.58 ± 0.04
Hyperoxic lungs	$1.43 \pm 0.15^*$	2.82 ± 0.52	$1.15 \pm 0.01^*$	$0.24 \pm 0.03^*$	$0.43 \pm 0.04^*$

$\bar{t}_c$, σ_c^2, RD$_c$ and Q$_c$ are the pulmonary capillary mean transit time, variance of capillary
transit times, relative dispersion of the capillary transit time distribution and the capillary
volume, respectively. Q$_v$ is the lung vascular volume. $\bar{t}_c$ values were estimated using
Equation (4.17). Values are mean $\pm$ SE. * indicates values that are significantly different
between normoxic (n = 9) and hyperoxic (n = 5) lungs (t-test; p < 0.05).
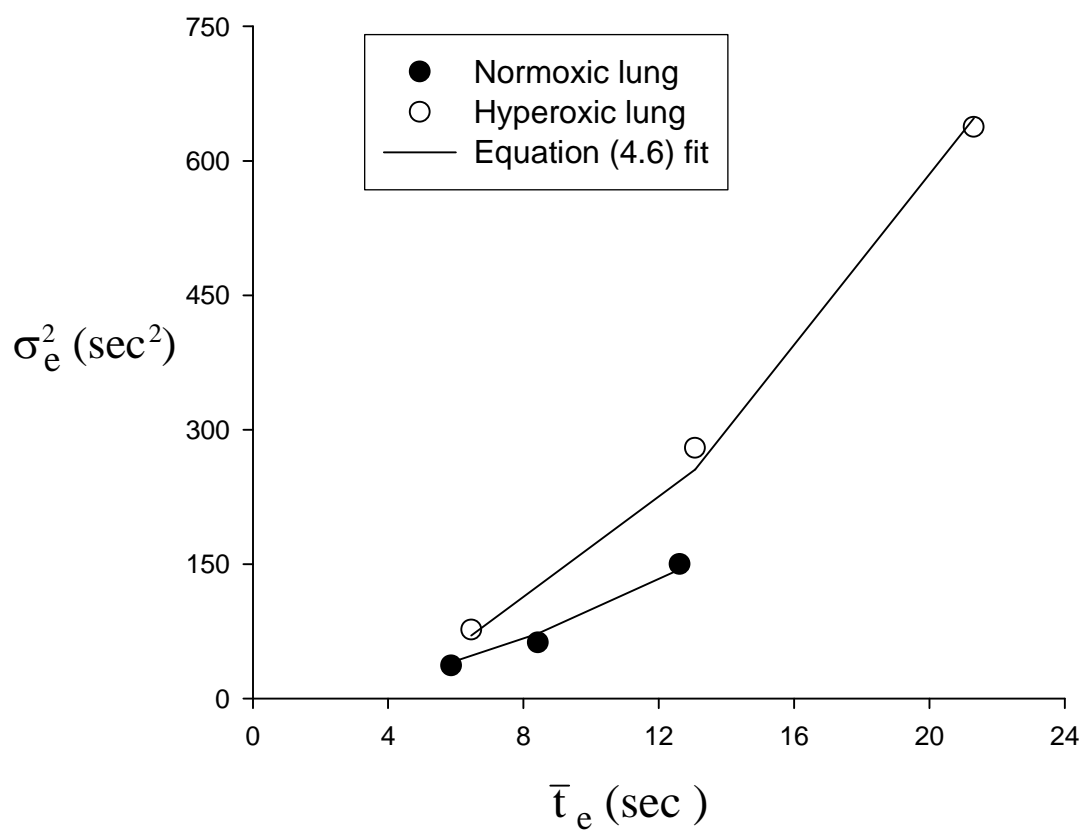
Figure 4.5: Symbols are data from the outflow curves shown in Figure (4.1) plotted according to Equation (4.17). $\bar{t}_e$ and σ_e^2 are CoQ_1H_2 extravascular mean residence time and variance, respectively. Solid lines are Equation (4.17) fit to the normoxic ($r^2 = 0.99$) and hyperoxic ($r^2 = 0.98$) data. The estimated value for $\bar{t}_c$ was ~2.45 and ~1.43 for normoxic and hyperoxic lungs respectively.

A random walk function (Equation (4.2)) was used to approximate the functional shape of the capillary transit time distribution for normoxic and hyperoxic lungs (Figure 4.6) using the average of the estimated values of the capillary mean transit times and variances in Table 4.5.
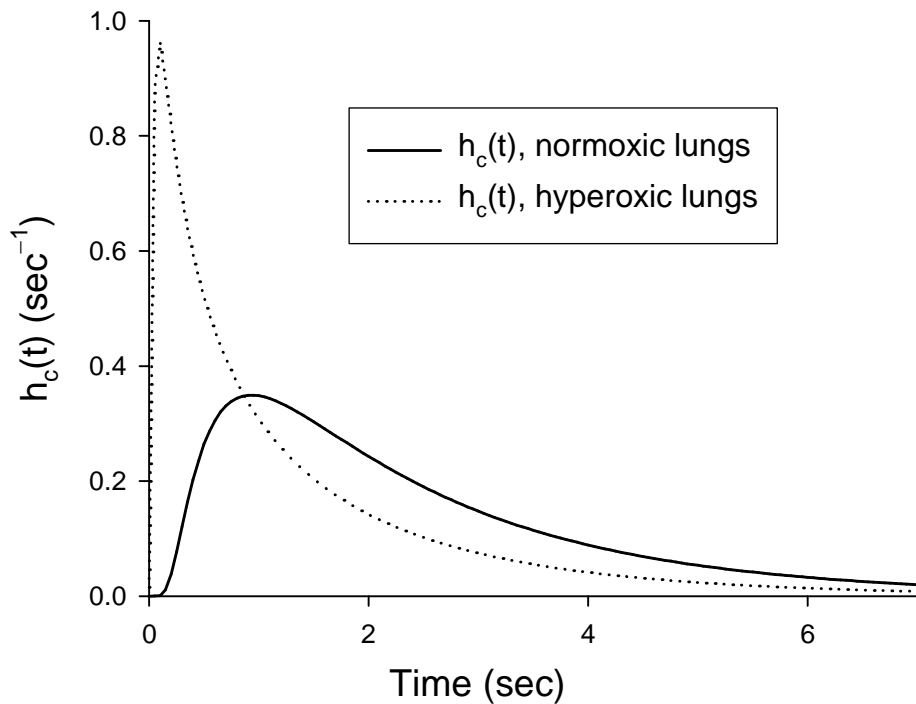
Figure 4.6: Functional form of the capillary transit time distribution for normoxic and hyperoxic lungs approximated using a shifted random walk function (Equation (4.2)) with the shift (t_s) set to zero.

5. SUMMARY, DISCUSSION AND CONCLUSIONS

The objective of this study was to evaluate the effect of rat exposure to hyperoxia (85% O_2 for 7 days) on the capillary mean transit time, $\bar{t}_c$, and the capillary transit time distribution, $h_c(t)$, in the intact rat lung using the multiple indicator dilution method developed by Audi et al. (Equations (4.11 a-b)) (Audi et al. 1994; Audi et al. 1995). The results demonstrate the utility of this method for determining $h_c(t)$, with CoQ_1H_2 as the flow-limited indicator, under the assumption that all of the variance of the lung vascular dispersion is due to the capillary bed. Moreover, the results suggest that rat exposure to this hyperoxia model decreases lung capillary mean transit time by ~42% and increases the heterogeneity of $h_c(t)$ by ~40%. In what follows, we discuss the results of this study, the limitations of the method, and draw some conclusions.

The method developed by Audi et al. for estimating $h_c(t)$ in the intact lung, referred to as **Method A** (Equations 4.11 a-b), requires the bolus injection of a vascular indicator and two rapidly equilibrating (or flow-limited) indicators with sufficiently different extravascular mean residence times ($\bar{t}_e$). Initial application of Method A, with CoQ_1H_2 at different perfusate BSA concentrations as the flow-limited indicators (Figure 4.1), revealed high correlation between σ_c^2 and $\bar{t}_c$. In other words, different combinations of σ_c^2 and $\bar{t}_c$ values gave similar fits (Table 4.3) based on Equations (4.12 a-b). To determine the reason for this high correlation, we carried out sensitivity analysis (Figure 4.4), which revealed that the two flow-limited indicators needed for applying method A should have $\bar{t}_e$ values that are not only sufficiently different, but also small enough relative to $\bar{t}_c$, such that $\bar{t}_e/\bar{t}_c$ is < 3 to break the correlation between $\bar{t}_c$ and σ_c^2 in

Equations (4.11 a-b). For the present study, the values of $\bar{t}_e$ for CoQ_1H_2 at the three

different perfusate BSA concentrations studied appear to be too high relative to $\bar{t}_c$,

especially for hyperoxic lungs, to be able to separately identify σ_c^2 and $\bar{t}_c$ based on

Equations (4.11a). Previous applications of Method A in isolated perfused dog lung

lobes, rabbit lungs and rat lungs done by Audi et al. utilized the lipophilic test indicators

diazepam and alfentanil, or diazepam at different perfusate albumin concentrations as the

flow-limited indicators (Audi et al. 1994; Audi et al. 1995). For those studies, the values

of $\bar{t}_e/\bar{t}_c$ ranged between 1 and 4 for the dog lung lobes, 1 and 3 for the rabbit lungs, and

1 and 2 for the normoxic rat lungs.

Previous studies in various species including normoxic rat lungs have suggested

that > 90% of the variance of the lung vascular dispersion is due to the capillary bed

(Audi et al. 2003; Audi et al. 1994; Audi et al. 1995; Clough et al. 1998). Thus, as an

alternative to Method A, we utilized **Method B1** (Audi et al. 1994; Audi et al. 1995) to

evaluate the effect of rat exposure to hyperoxia on lung $h_c(t)$. Method B1, which is a

simplified version of Method A, assumes that all the variance of the lung vascular

dispersion is due to the capillary bed (Audi et al. 1994; Audi et al. 1995). Under this

assumption, σ_c^2 is fixed to σ_V^2, which is the difference between the variances of the

outflow curves measured following bolus injections of FITC-dex with and without the

lung connected to the perfusion system (Equation (4.7)). With σ_c^2 known, the moments of

the outflow curve of one flow-limited indicator (CoQ_1H_2) would be sufficient to estimate

$\bar{t}_c$ using Equation (4.16).

Table 5.1 summarizes previous estimates of the pulmonary capillary mean transit

time ($\bar{t}_c$) capillary volume ($Q_c = F \cdot \bar{t}_c$), and relative dispersion (RD_c) of $h_c(t)$ for the

normoxic rat lung for comparison with the present study. To put this comparison in

perspective, it is useful to compare Q_c, which is less dependent on the flow (F) than is $\bar{t}_c$.

Table 5.1: Estimates of pulmonary capillary perfusion parameters for normoxic rat lungs in chronological order

Method	Body wt, g	Q_c, ml	Q_c ml/kg Body wt	Flow ml/min	$\bar{t}_c$, s	RD_c	Reference
Morphometric	363 ± 4	0.66 ± 0.06	1.82				(Crapo et al. 1980)
Morphometric	366 ± 4	0.71 ± 0.06	1.94				(Sjostrom and Crapo 1983)
Morphometric	224	0.58 ± 0.05	2.6				(Randell, Mercer, and Young 1990)
Fluorescence microscopy	360 - 580	0.49 ± 0.03	1.04	7.5	3.9 ± 0.2	0.57 ± 0.02	(Presson et al. 1997)
Morphometric	306 ± 5	0.51 ± 0.05	1.67				(Howell, Preston, and McLoughlin 2003)
MID Method A	323 ± 6	0.47 ± 0.02	1.46	30	0.94 ± 0.04	0.91 ± 0.03	(Audi et al. 2003)
Present method (Method B1)	292 ± 9	0.41 ± 0.04	1.40	10	2.45 ± 0.24	0.82 ± 0.03	Present study

Estimates of pulmonary capillary blood volume (Q_c), mean transit time ($\bar{t}_c$), and relative dispersion (RD_c) of $h_c(t)$. Values are mean ± SE.

Table 5.1 shows that the capillary volume estimated in the present study is close

to that estimated by (Audi et al. 2003) using Method A with ^{3}H-alfentanil and [14]C-

diazepam as the flow-limited indicators, and to the capillary volume estimated by

(Presson et al. 1997) using subpleural vessel fluorescence video-microscopy under

similar flow conditions. However, Table 5.1 shows that the morphometric estimates of

the capillary volume (0.58 to 0.71 ml) are higher than those estimated in the present study

or by using subpleural vessel fluorescence video-microscopy (Crapo et al. 1980; Randell,

Mercer, and Young 1990; Sjostrom and Crapo 1983). This is not surprising, since

morphometric estimates of capillary volume have sometimes been considered to be close

to the maximum value, which might not be achieved when the pulmonary blood flow and

vascular pressures are low, as is the case in the present study (Audi et al. 1994; Audi et

al. 1995).

The estimated relative dispersion (RD_c) of the capillary transit time distribution

for normoxic lungs, 0.82 ± 0.03 (SE), in the present study (Table 4.2) is close to that

estimated by (Audi et al. 2003) using method A with ^{3}H-alfentanil and ^{14}C-diazepam as

the flow-limited indicators (0.91 ± 0.03), but smaller than that estimated using subpleural

vessel fluorescence video-microscopy (0.57 ± 0.02) under similar flow conditions

(Presson et al. 1997). This could be, in part, due to morphometric differences between

subpleural and intrapulmonary capillary beds (Guntheroth, Luchtel, and Kawabori 1982;

Miller 1947), although Presson et al. suggested that these differences might not be

significant for the rat lung (Presson et al. 1997).

Table 4.3 shows that rat exposure to hyperoxia (85% O_2 for 7 days) decreased the

lung capillary volume by more than 40% from 0.41 ± 0.04 (SE) ml to 0.24 ± 0.03 ml.

This result is consistent with that measured by (Crapo et al. 1980) using a morphometric

method. They showed that rat exposure to 85% O_2 for 7 days decreased the capillary

volume by ~53% from 0.66 ± 0.06 (SE) ml to 0.31 ± 0.04 ml. This hyperoxia-induced

decrease in capillary volume is also consistent with the hyperoxia-induced ~58%

decrease in rate (PS) of ACE-mediated FAPGG hydrolysis measured in the present study

(Table 3.2). Assuming no change in ACE activity per unit surface area between normoxic and hyperoxic lungs, the estimated PS value (Table 3.2) would be a measure of perfused surface area (Audi et al. 2003; Audi et al. 2008). The ~58% hyperoxia-induced decrease in PS product (Table 3.2) is consistent with the ~50% decrease in surface area of the capillary endothelium measured by Crapo et al. using morphometric methods (4524 ± 324 (SE) cm^2 vs. 2289 ± 269 cm^2) (Crapo et al. 1980).

The results of the present study suggest that rat exposure to hyperoxia not only decreased the capillary volume, but also increased the relative dispersion of $h_c(t)$ by ~40% from 0.82 ± 0.03 (SE) to 1.15 ± 0.01 for normoxic and hyperoxic lungs, respectively. To our knowledge, this is the first study to evaluate the effect of rat exposure to 85% O_2 for 7 days on the heterogeneity of $h_c(t)$. This hyperoxia-induced increase in the RD_c is revealed in the measured CoQ_1H_2 and FITC-dex outflow curves (Figures 3.2) as a decrease in the shift of the peaks of CoQ_1H_2 relative to that for the FITC-dex curve as demonstrated by model simulations described next.

To evaluate the effect of an increase in the heterogeneity of $h_c(t)$ on the extent of shift between the peaks of the outflow curves of a vascular indicator and a flow-limited indicator, two lung models (Appendix B) were created to simulate the outflow curves of the vascular and flow-limited indicators following their arterial bolus injections in a normoxic lung (normoxic model) and a hyperoxic lung (hyperoxic model). For the normoxic model, the values of $\bar{t}_c$ and RD_c were set at 2.5 sec and 0.8, respectively. For the hyperoxic model, the value of RD_c was set 1.2, while the value of $\bar{t}_c$ was set as that for the normoxic model (2.5 sec). For both models, the values of $\bar{t}_e$ for the flow-limited indicators were set at 4, 8 and 12 sec. Moreover, both models were assumed to have the

same level of bolus dispersion outside the capillary bed (tubing and conducting vessels).

Figure 5.1 shows the simulated outflow curves of vascular and flow-limited indicators

from the normoxic model (panel a.) and hyperoxic model (panel b.).
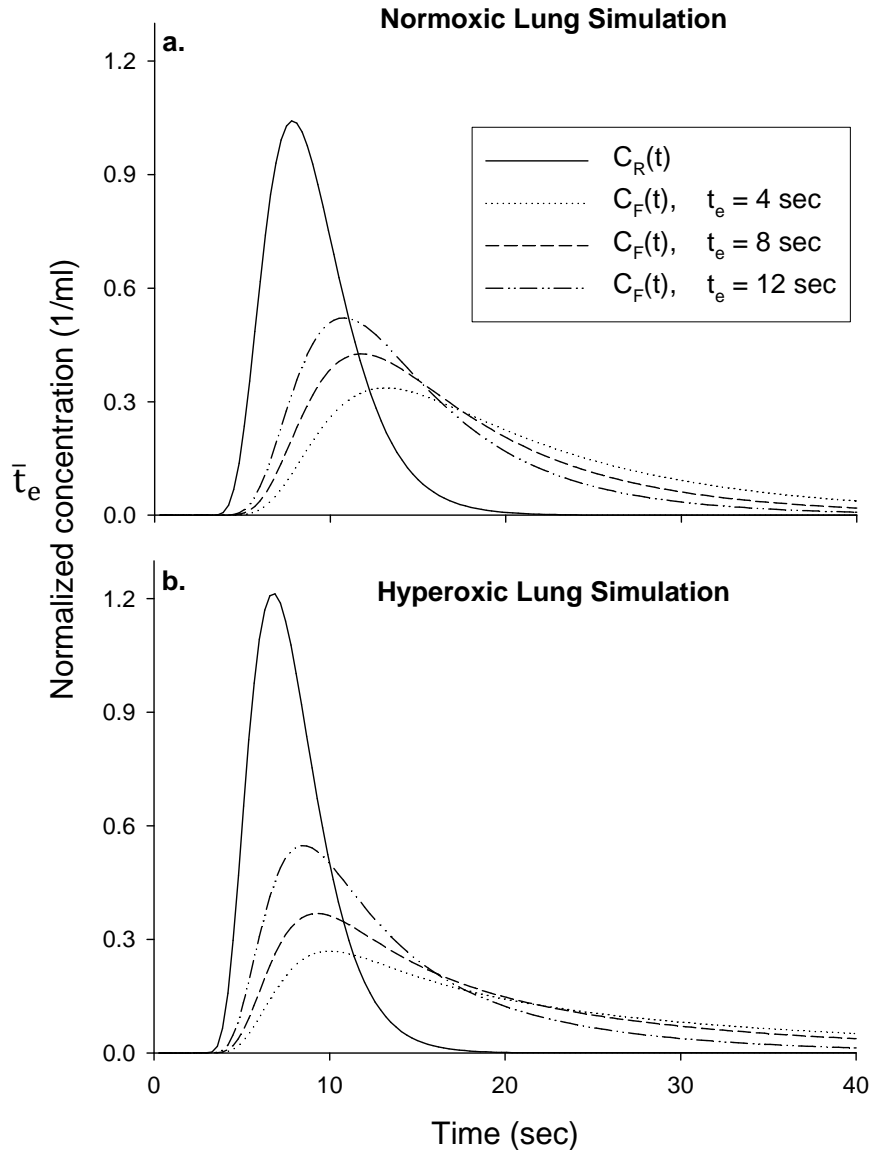
Figure 5.1: Simulations (see Appendix B) of arterial bolus injections of a vascular indicator ($C_R(t)$) and three flow-limited ($C_F(t)$) indicators with different extravascular mean residence times ($\bar{t}_e$) in a normoxic (panel a.) and a hyperoxic (panel b.) lung. The normoxic and hyperoxic model simulations are assumed to have the same bolus dispersion outside the capillary bed, same capillary mean transit time, but different capillary relative dispersions ($RD_c = 0.8$ and 1.2 for normoxic and hyperoxic lungs simulations, respectively).

Figure 5.1 shows that all else being equal, increasing the heterogeneity of $h_c(t)$ decreases the shift between the peaks of the outflow curves of the vascular indicator and flow-limited indicators.

The simulated concentration versus time outflow curves shown in Figure 5.1 (panel a.) were also used to evaluate the effect of vascular dispersion outside the capillary bed on the estimated value of $\bar{t}_c$ using Method B1 (Equation (4.16)) which assumes that the variance of the lung vascular dispersion is due to the capillary bed. The moments of each of the simulated outflow curves were estimated and Equation (4.16) was then used to estimate $\bar{t}_c$ with σ_v^2 set at the actual value of σ_c^2, at 1.1 times the actual value of σ_c^2 (10% overestimation of σ_c^2), and at 1.2 times the actual value of σ_c^2 (20% overestimation of σ_c^2). Figure 5.2 shows the ratios of estimated (Equation (4.16)) to actual values of $\bar{t}_c$ as a function of σ_v^2/σ_c^2. Overestimation of σ_c^2 by 10% and 20% resulted on average in overestimation of $\bar{t}_c$ by ~ 7% and ~15%, respectively.

Table 4.1 shows the estimated values of the vascular volume and vascular relative dispersion in normoxic and hyperoxic lungs. The estimated vascular volume of 0.70 ± 0.04 ml in the present study is similar to that estimated previously (0.75 ± 0.05 (SE) ml) under similar flow conditions (10 ml/min) (Audi et al. 2005), but about 17% lower than that estimated (0.85 ± 0.06 (SE) ml) at a flow of 30 ml/min (Audi et al. 2003). To determine whether passive distension of blood vessels resulting from the higher perfusion pressure (~10 Torr) at 30 ml/min compared to a perfusion pressure of ~5 Torr at 10 ml/min could account for this difference in vascular volume, we carried out the following analysis.
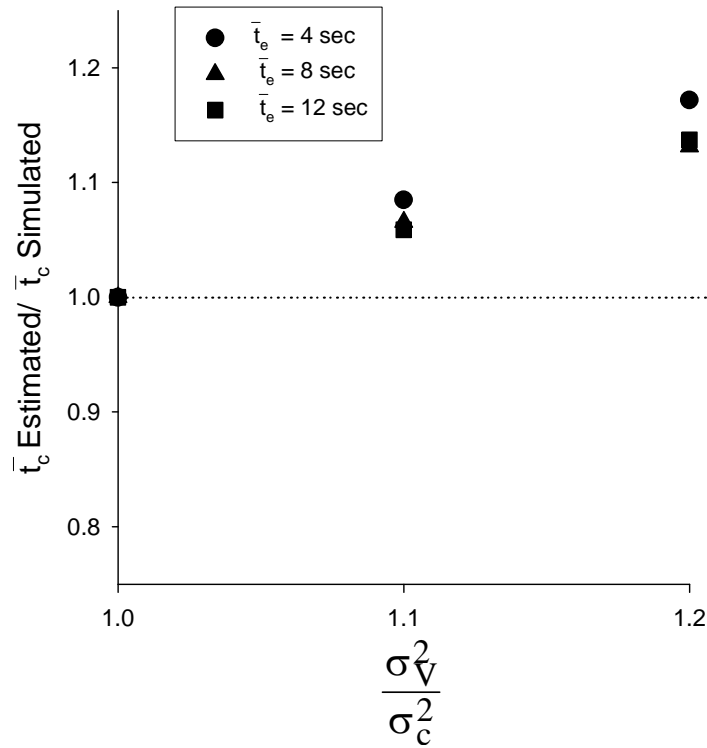
Figure 5.2: Ratio of estimated value (Estimated) of capillary mean transit time ($\bar{t}_c$) using Equation (4.17) to that used in the simulations (Simulated) as a function of the ratio of total vascular variance (σ_v^2) to the capillary variance (σ_c^2) for three different extravascular mean residence times ($\bar{t}_e$). The values of $\bar{t}_c$ and σ_c^2 used in the model simulations were 2.5 sec and 4 sec^2, respectively. The values of extravascular mean residence times ($\bar{t}_e$) were 4.0, 8.0, and 12.0 sec.

Let us start by assuming a linear relationship between vessel diameter (D),

transpulmonary pressure (P_t) and distensibility coefficient (α).

$$D_2 = D_1 (1 + \alpha (P_{t2} - P_{t1})) \qquad\qquad (5.1)$$

where D_1 and D_2 are the vessel diameters at pressures P_{t1} and P_{t2}, respectively (Ahuja

2007). Assuming the value of P to be the average of the arterial and venous pressures (~0

Torr), a constant α of 2.8 % per Torr and a cylindrical model for arteries, capillaries and

veins (Karau et al. 2001), Equation (5.1) predicts an 8.0 % increase in diameter due to a 2.5 Torr increase in pressure. This increase in diameter would translate to ~17 % increase in volume which is equal to the ~17 % increase in vascular volume. Recent unpublished data from Dr. Molthen's lab (Zablocki VA Medical Center, Milwaukee, WI) revealed no significant difference in α between normoxic (2.70 %) and hyperoxic (2.67 %) rat lungs. Thus, virtually all of the difference in the measured total vascular volume at 10 and 30 ml/min could be accounted for by passive distension of the blood vessels.

Rat exposure to hyperoxia decreased lung vascular volume by ~21%, with no significant effect on the relative dispersion of lung vascular transit time distribution (Table 4.1). This decrease in vascular volume is revealed experimentally by a decrease in the peak of the FITC-dex outflow curve measured following the bolus injection of FITC-dex with the lung connected to the perfusion system (Figure 3.2). This hyperoxia-induced decrease in vascular volume (~0.15 ml) (Table 4.1) is comparable to the hyperoxia-induced decrease in capillary volume (~0.17 ml) (Table 4.5), which suggests that exposure to hyperoxia had no significant effect on the volume of the conducting vessels of the lung. As a result, the capillary volume as a percentage of the vascular volume decreased from 58 ± 4 (SE) % in normoxic lungs to 43 ± 4 % in hyperoxic lungs.

Method B1 is equivalent to the superposition method developed by (Goresky 1963) as implemented by (Audi et al. 1995). Thus, one would expect the estimates of $\bar{t}_c$ using the Goresky superposition method to be comparable to those estimated using Method B1, if the dispersion due to the tubing, injection, and sampling systems were removed from the FITC-dex and CoQ_1H_2 outflow curves measured in presence of the lung before applying the superposition method (Audi et al. 1995). Thus, application of

the superposition method would require deconvolution of the FITC-dex curve measured with the lung removed from the perfusion system from the CoQ_1H_2 and FITC-dex curves measured with the lung connected to the perfusion system (Figure 4.3).

The use of high CoQ_1H_2 concentration (1200 μM) in the present study was to increase the signal-to-noise ratio in the tails of the measured venous effluent concentration versus time outflow curves following the arterial bolus injection of CoQ_1H_2 (Figure 3.2). One of the underlying assumptions of this study and Equation (4.5) is that CoQ_1H_2 binding to perfusate BSA is not saturable, and hence, follows first order kinetics (Audi et al. 2008). The results in Figure 4.2 are consistent with this assumption. To further evaluate this assumption, in one normoxic lung perfused with 3% BSA perfusate, we measured the CoQ_1H_2 venous effluent outflow curves following the arterial injection of two boluses, one containing 800 μM CoQ_1H_2 and another containing 1200 μM CoQ_1H_2. Figure 5.3 shows that the normalized CoQ_1H_2 concentration versus time outflow curves for the 800 μM and 1200 μM bolus injections are virtually superimposable, which is consistent with the assumption that CoQ_1H_2 binding to BSA is not saturable.

Comparison of the results from the present study with previous results using Method A in the isolated perfused dog lung lobe and rabbit lungs reveals quantitative differences in the estimated vascular and capillary mean transit times among these species (Audi et al. 1994; Audi et al. 1995). Assuming a normal cardiac output of 2.9 liter/min for a 20-kg dog, Audi et al. estimated that the pulmonary capillary and the total pulmonary vascular mean transit times would be ~1.62 and 3.4 sec, respectively (Audi et al. 1994).
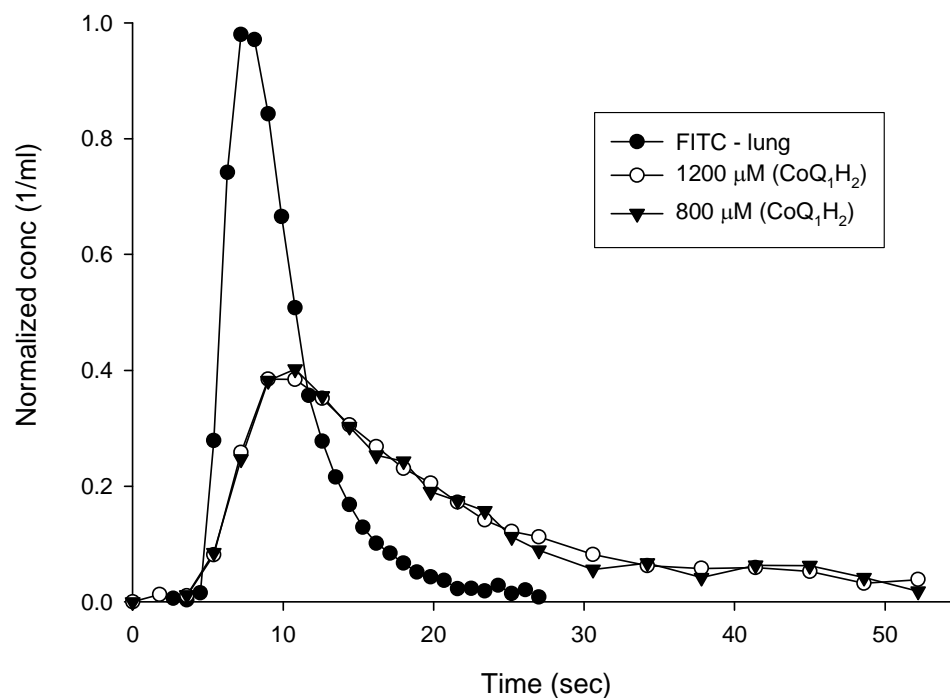
Figure 5.3: Normalized concentration versus time outflow curves obtained following arterial bolus injections of FITC-dex and CoQ_1H_2 at concentrations of 800 µM and 1200 µM in a normoxic rat lung.

For a 2.7 kg rabbit with a normal cardiac output of 340 ml/min, the estimated pulmonary capillary and the total pulmonary vascular mean transit times by Audi et al. are ~0.76 and 1.7 sec, respectively (Audi et al. 1995). Assuming a normal cardiac output of 75 ml/min for a 300 g rat (Presson et al. 1997), the estimated pulmonary capillary and the total pulmonary vascular mean transit times in the present study based on the results in Tables 4.4 would be 0.34 and 0.57 sec, respectively, without accounting for the effect of passive distension of blood vessels at higher flow. These values appear to be substantially shorter than those for the rabbit, which in turn are substantially shorter than those for the dog. However, the pulmonary capillary mean transit time as a percentage of the total vascular mean transit time appears to be similar for dogs (48%), rabbits (44%) and rats (60%).

Figure 5.4 shows a linear relationship between total vascular mean transit time and capillary mean transit times for dog, rabbit and rat lungs. Thus, the shorter capillary mean transit time in the rat as compared to those for the rabbit and dog may be primarily attributed to proportionately shorter total vascular mean transit times. Moreover, studies by Staub et al. (Staub and Schultz 1968) and Mercer et al. (Mercer and Crapo 1987) show that the capillary length in rat lungs (~ 205 μm) was significantly shorter than in rabbit lungs (550-650 μm) and dog lungs (600-800 μm).

The rat lung capillary mean transit time reported in the present study is plasma mean transit time, which is generally longer than that of red blood cells because of the Fahraeus effect (Albrecht et al. 1979; Presson et al. 1997). Presson et al. found the plasma mean transit time in subpleural capillaries of dog lungs to be ~40% longer than that for RBC (Presson et al. 1995). Assuming similar capillary velocities and diameters for capillaries in the rat lung, the estimated RBC mean transit time based on the results of the present study would be ~0.24 sec, which is close to the ~0.25 sec time needed for O_2 to diffuse and react with RBCs (Presson et al. 1997). This suggests that rat lungs have no reserve capillary RBC mean transit time as compared to dogs (1.2 sec) and rabbits (0.6 sec). This could be in part due to the fact that the estimated plasma capillary mean transit time in the present study does not account for capillary distension due to difference in lung perfusion pressure at normal cardiac output (~75 ml/min for 300 g rat) as compared to 10 ml/min perfusate flow used in the present study. Another reason for this small capillary RBC mean transit time reserve for rats as compared to dogs could be the relatively short lung capillary length and resting capillary mean transit time for rats as compared to dogs (Mercer and Crapo 1987; Staub and Schultz 1968). The apparent low

reserve lung RBC capillary mean transit time for rats is also consistent with the fact that small species like rats, which have relatively high resting metabolic rates, can only increase their O_2 consumption by 3-fold as compared to 25-fold for dogs (Presson et al. 1997).
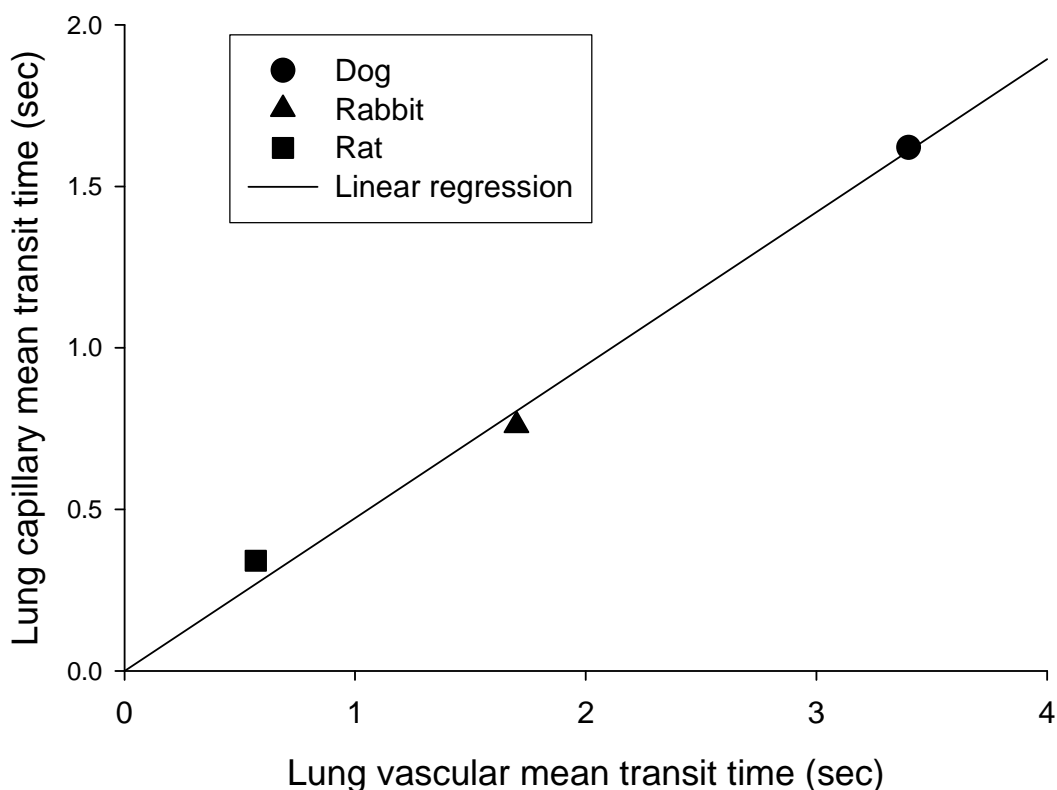
Figure 5.4: Lung capillary mean transit time ($\bar{t}_c$) plotted as a function of the total lung vascular mean transit time ($\bar{t}_v$) in dog, rabbit and rat. Solid line represents a linear regression fit (with zero intercept) to the data ($r^2 = 0.99$).

Previous studies have shown that rat exposure to 85% O_2 for 7 days confers tolerance to the otherwise lethal effects of exposure to > 95% O_2 (Crapo et al. 1980; Sjostrom and Crapo 1983). Understanding the underlying mechanisms of rat tolerance or susceptibility to > 95% O_2 may lead to the identification of potential therapeutic targets

for protection from O_2 toxicity. Additional studies would be needed to determine whether the hyperoxia-induced decrease in capillary volume and increase in the heterogeneity (RD_c) of $h_c(t)$ measured in the present study are important to the hyperoxia-induced tolerance to > 95% O_2. For instance, neutrophils have been shown to play a role in the pathogenesis of lung O_2 toxicity and neutrophil depletion has been shown to be protective against hyperoxic lung injury (Auten, Whorton, and Nicholas Mason 2002). The measured hyperoxia-induced decrease in lung capillary mean transit time and increase in RD_c may affect the retention or margination of neutrophils on passage through the capillary bed (Brown et al. 1995). However, Crapo et al. showed an increase in the number of neutrophils in the interstitial space of lungs of rats exposed to 85% O_2 for 7 days as compared to normoxic rat lungs (Crapo et al. 1980). Analysis of the kinetics of neutrophil transit through the lungs of hyperoxic rats would be needed to measure the effect of decrease in $\bar{t}_c$ and increase in RD_c on neutrophil retention in the pulmonary capillary bed.

Sjostrom et al. demonstrated that rats exposed to hypoxia (10 to 11% O_2) for 7 days also develop tolerance to the otherwise lethal effects of > 95% O_2 (Sjostrom and Crapo 1983). However, unlike exposure to 85% O_2 for 7 days, which results in the loss of more than half of the surface area of the capillary endothelium, exposure to hypoxia has no significant effect on the surface area of the pulmonary capillary endothelium (Sjostrom and Crapo 1983). This may suggest that the decrease in lung capillary mean transit time in lungs of rats exposed to 85% O_2 for 7 days is not important for the acquired tolerance to > 95% O_2. The proposed method for measuring $h_c(t)$ could be used to evaluate the effect of rat exposure to hypoxia on the heterogeneity of $h_c(t)$.

In conclusion, the results of this study demonstrate that estimates of the rat lung capillary transit time distribution can be obtained from the venous effluent concentration versus time outflow curves of a vascular indicator and one flow-limited indicator such as CoQ_1H_2, measured following the arterial bolus injection of these indicators. Furthermore, the results reveal that rat exposure to hyperoxia decreased the capillary mean transit time and increased the heterogeneity of the capillary transit time distribution. These results are important for subsequent evaluation of the effect of hyperoxia on the activities of pro- and anti-oxidant redox enzymes in the intact lung using indicator dilution methods. For instance, preliminary indicator dilution studies in Dr. Audi's laboratory have demonstrated that rat exposure to this hyperoxia model alters the capacity of the rat lung to metabolize the test indicators CoQ_1, DQ, DQH_2 and CoQ_1H_2 on their passage through the pulmonary circulation. The hyperoxia-induced change in lung capillary perfusion kinematics measured in the present study can alter the redox metabolism of these test indicators on passage through the lung. Thus, proper interpretation of the resulting indicator dilution data in terms of the effect of hyperoxia on the lung activities of the redox enzymes (NQO1 and mitochondrial complexes I and III) with which these test indicators interact on passage through the lung requires accounting for the effect of hyperoxia on lung capillary perfusion kinematics in the mathematical model used to quantify this data.

BIBLIOGRAPHY

Ahuja, T. 2007. Quantification of pulmonary perfusion kinematics in rats from microfocal angiographic images. Master's Thesis, Marquette University.

Albrecht, K. H., P. Gaehtgens, A. Pries, and M. Heuser. 1979. The fahraeus effect in narrow capillaries (i.D. 3.3 to 11.0 micron). *Microvasc Res* 18, no. 1: 33-47.

Audi, S. H. 1993. Estimation of pulmonary capillary volume and endothelium barrier function using multiple indicator dilution method. Ph.D Dissertation, Marquette University.

Audi, S. H., R. D. Bongard, C. A. Dawson, D. Siegel, D. L. Roerig, and M. P. Merker. 2003. Duroquinone reduction during passage through the pulmonary circulation. *Am J Physiol Lung Cell Mol Physiol* 285, no. 5: L1116-31.

Audi, S. H., R. D. Bongard, G. S. Krenz, D. A. Rickaby, S. T. Haworth, J. Eisenhauer, D. L. Roerig, and M. P. Merker. 2005. Effect of chronic hyperoxic exposure on duroquinone reduction in adult rat lungs. *Am J Physiol Lung Cell Mol Physiol* 289, no. 5: L788-97.

Audi, S. H., R. D. Bongard, Y. Okamoto, M. P. Merker, D. L. Roerig, and C. A. Dawson. 2001. Pulmonary reduction of an intravascular redox polymer. *Am J Physiol Lung Cell Mol Physiol* 280, no. 6: L1290-9.

Audi, S. H., C. A. Dawson, S. B. Ahlf, and D. L. Roerig. 2001. Oxygen dependency of monoamine oxidase activity in the intact lung. *Am J Physiol Lung Cell Mol Physiol* 281, no. 4: L969-81.

Audi, S. H., C. A. Dawson, S. B. Ahlf, and D. L. Roerig. 2002. Lung tissue mitochondrial benzodiazepine receptors increase in a model of pulmonary inflammation. *Lung* 180, no. 5: 241-50.

Audi, S. H., C. A. Dawson, J. H. Linehan, G. S. Krenz, S. B. Ahlf, and D. L. Roerig. 1996. An interpretation of 14c-urea and 14c-primidone extraction in isolated rabbit lungs. *Ann Biomed Eng* 24, no. 3: 337-51.

Audi, S. H., G. S. Krenz, J. H. Linehan, D. A. Rickaby, and C. A. Dawson. 1994. Pulmonary capillary transport function from flow-limited indicators. *J Appl Physiol* 77, no. 1: 332-51.

Audi, S. H., J. H. Linehan, G. S. Krenz, and C. A. Dawson. 1998. Accounting for the heterogeneity of capillary transit times in modeling multiple indicator dilution data. *Ann Biomed Eng* 26, no. 6: 914-30.

Audi, S. H., J. H. Linehan, G. S. Krenz, C. A. Dawson, S. B. Ahlf, and D. L. Roerig. 1995. Estimation of the pulmonary capillary transport function in isolated rabbit lungs. *J Appl Physiol* 78, no. 3: 1004-14.

Audi, S. H., Linehan, J. H., Krenz, G. S., Roerig, S. B., Roerig, D. L., Ahlf, S. B. and Dawson, C. A. 1998. Lipophilic amines as probes for measurement of lung capillary transport function and tissue composition using the multiple-indicator dilution method. In *Whole organ approaches to cellular metabolish: Permeation, cellular uptake, and product formation*, ed. J. B. Bassingthwaighte, Goresky, C. A. and Linehan J. H.:517 - 543. New York: Springer.

Audi, S. H., M. P. Merker, G. S. Krenz, T. Ahuja, D. L. Roerig, and R. D. Bongard. 2008. Coenzyme q1 redox metabolism during passage through the rat pulmonary circulation and the effect of hyperoxia. *J Appl Physiol* 105, no. 4: 1114-26.

Audi, S. H., L. E. Olson, R. D. Bongard, D. L. Roerig, M. L. Schulte, and C. A. Dawson. 2000. Toluidine blue o and methylene blue as endothelial redox probes in the intact lung. *Am J Physiol Heart Circ Physiol* 278, no. 1: H137-50.

Auten, R. L., M. H. Whorton, and S. Nicholas Mason. 2002. Blocking neutrophil influx reduces DNA damage in hyperoxia-exposed newborn rat lung. *Am J Respir Cell Mol Biol* 26, no. 4: 391-7.

Bassingthwaighte, J. B. and M. Chaloupka. 1984. Sensitivity functions in the estimation of parameters of cellular exchange. *Fed Proc* 43, no. 2: 181-4.

Bassingthwaighte, J. B.; Goresky, CA; Linehan, JH. 1998. *Whole organ approaches to cellular metabolism: Permeation, cellular uptake, and product formation*. New York: Springer.

Bhandari, V., R. Choo-Wing, C. G. Lee, Z. Zhu, J. H. Nedrelow, G. L. Chupp, X. Zhang, M. A. Matthay, L. B. Ware, R. J. Homer, P. J. Lee, A. Geick, A. R. de Fougerolles, and J. A. Elias. 2006. Hyperoxia causes angiopoietin 2-mediated acute lung injury and necrotic cell death. *Nat Med* 12, no. 11: 1286-93.

Brown, G. M., D. M. Brown, K. Donaldson, E. Drost, and W. MacNee. 1995. Neutrophil sequestration in rat lungs. *Thorax* 50, no. 6: 661-7.

Brueckl, C., S. Kaestle, A. Kerem, H. Habazettl, F. Krombach, H. Kuppe, and W. M. Kuebler. 2006. Hyperoxia-induced reactive oxygen species formation in pulmonary capillary endothelial cells in situ. *Am J Respir Cell Mol Biol* 34, no. 4: 453-63.

Cadenas, E. 1995. Antioxidant and prooxidant functions of dt-diaphorase in quinone metabolism. *Biochem Pharmacol* 49, no. 2: 127-40.

Capellier, G., V. Maupoil, S. Boussat, E. Laurent, and A. Neidhardt. 1999. Oxygen toxicity and tolerance. *Minerva Anestesiol* 65, no. 6: 388-92.

Chan, T. S., S. Teng, J. X. Wilson, G. Galati, S. Khan, and P. J. O'Brien. 2002. Coenzyme q cytoprotective mechanisms for mitochondrial complex i cytopathies involves nad(p)h: Quinone oxidoreductase 1(nqo1). *Free Radic Res* 36, no. 4: 421-7.

Clough, A. V., A. al-Tinawi, J. H. Linehan, and C. A. Dawson. 1994. Regional transit time estimation from image residue curves. *Ann Biomed Eng* 22, no. 2: 128-43.

Clough, A. V., S. T. Haworth, C. C. Hanger, J. Wang, D. L. Roerig, J. H. Linehan, and C. A. Dawson. 1998. Transit time dispersion in the pulmonary arterial tree. *J Appl Physiol* 85, no. 2: 565-74.

Clough, A. V., J. H. Linehan, and C. A. Dawson. 1997. Regional perfusion parameters from pulmonary microfocal angiograms. *Am J Physiol* 272, no. 3 Pt 2: H1537-48.

Crapo, J. D. 1975. Superoxide dismutase and tolerance to pulmonary oxygen toxicity. *Chest* 67, no. 2 Suppl: 39S-40S.

Crapo, J. D., B. E. Barry, H. A. Foscue, and J. Shelburne. 1980. Structural and biochemical changes in rat lungs occurring during exposures to lethal and adaptive doses of oxygen. *Am Rev Respir Dis* 122, no. 1: 123-43.

Crapo, J. D. and D. F. Tierney. 1974. Superoxide dismutase and pulmonary oxygen toxicity. *Am J Physiol* 226, no. 6: 1401-7.

Dawson, C. A., S. H. Audi, R. D. Bongard, Y. Okamoto, L. Olson, and M. P. Merker. 2000. Transport and reaction at endothelial plasmalemma: Distinguishing intra- from extracellular events. *Ann Biomed Eng* 28, no. 8: 1010-8.

Dawson, C. A., S.H. Audi, G.S. Krenz, and D.L. Roerig. 2003. Endothelium and compound transfer. In *Molecular nuclear medicine: The challenge of genomics and proteomics to clinical practice*, ed. L.E.; Shreeve Feinendegen, W.W.; Eckelman, W.C.; Bahk, Y.W.; and Wagner, Jr., H.N.:201-216. New York: Springer.

Di Virgilio, F. and G. F. Azzone. 1982. Activation of site i redox-driven h+ pump by exogenous quinones in intact mitochondria. *J Biol Chem* 257, no. 8: 4106-13.

Evelson, P. and B. Gonzalez-Flecha. 2000. Time course and quantitative analysis of the adaptive responses to 85% oxygen in the rat lung and heart. *Biochim Biophys Acta* 1523, no. 2-3: 209-16.

Fato, R., E. Estornell, S. Di Bernardo, F. Pallotti, G. Parenti Castelli, and G. Lenaz. 1996. Steady-state kinetics of the reduction of coenzyme q analogs by complex i (nadh:Ubiquinone oxidoreductase) in bovine heart mitochondria and submitochondrial particles. *Biochemistry* 35, no. 8: 2705-16.

Fisher, A. B. and M. F. Beers. 2008. Hyperoxia and acute lung injury. *Am J Physiol Lung Cell Mol Physiol* 295, no. 6: L1066; author reply L1067.

Fisher, A.B. 1987. Oxygen utilization and toxicity in the lungs. In *Handbook of physiology: The respiratory system*, ed. A.P. Fishman:231-254. Bethesda: Williams & Wilkins.

Frank, L., J. Iqbal, M. Hass, and D. Massaro. 1989. New "rest period" protocol for inducing tolerance to high o2 exposure in adult rats. *Am J Physiol* 257, no. 4 Pt 1: L226-31.

Freeman, B. A. and J. D. Crapo. 1982. Biology of disease: Free radicals and tissue injury. *Lab Invest* 47, no. 5: 412-26.

Freeman, B. A., M. K. Topolosky, and J. D. Crapo. 1982. Hyperoxia increases oxygen radical production in rat lung homogenates. *Arch Biochem Biophys* 216, no. 2: 477-84.

Glenny, R. W., S. L. Bernard, and H. T. Robertson. 2000. Pulmonary blood flow remains fractal down to the level of gas exchange. *J Appl Physiol* 89, no. 2: 742-8.

Goresky, C. A. 1963. A linear method for determining liver sinusoidal and extravascular volumes. *Am J Physiol* 204: 626-40.

Guntheroth, W. G., D. L. Luchtel, and I. Kawabori. 1982. Pulmonary microcirculation: Tubules rather than sheet and post. *J Appl Physiol* 53, no. 2: 510-5.

Hayatdavoudi, G., J. J. O'Neil, B. E. Barry, B. A. Freeman, and J. D. Crapo. 1981. Pulmonary injury in rats following continuous exposure to 60% o2 for 7 days. *J Appl Physiol* 51, no. 5: 1220-31.

Heffner, J. E. and J. E. Repine. 1989. Pulmonary strategies of antioxidant defense. *Am Rev Respir Dis* 140, no. 2: 531-54.

Ho, Y. S., M. S. Dey, and J. D. Crapo. 1996. Antioxidant enzyme expression in rat lungs during hyperoxia. *Am J Physiol* 270, no. 5 Pt 1: L810-8.

Howell, K., R. J. Preston, and P. McLoughlin. 2003. Chronic hypoxia causes angiogenesis in addition to remodelling in the adult rat pulmonary circulation. *J Physiol* 547, no. Pt 1: 133-45.

Jackson, R. M. 1985. Pulmonary oxygen toxicity. *Chest* 88, no. 6: 900-5.

Jamieson, D., B. Chance, E. Cadenas, and A. Boveris. 1986. The relation of free radical production to hyperoxia. *Annu Rev Physiol* 48: 703-19.

Johnson, C. R., Y. Guo, E. S. Helton, S. Matalon, and R. M. Jackson. 1998. Modulation of rat lung na+,k(+)-atpase gene expression by hyperoxia. *Exp Lung Res* 24, no. 2: 173-88.

Karau, K. L., R. H. Johnson, R. C. Molthen, A. H. Dhyani, S. T. Haworth, C. C. Hanger, D. L. Roerig, and C. A. Dawson. 2001. Microfocal x-ray ct imaging and pulmonary arterial distensibility in excised rat lungs. *Am J Physiol Heart Circ Physiol* 281, no. 3: H1447-57.

Kimball, R. E., K. Reddy, T. H. Peirce, L. W. Schwartz, M. G. Mustafa, and C. E. Cross. 1976. Oxygen toxicity: Augmentation of antioxidant defense mechanisms in rat lung. *Am J Physiol* 230, no. 5: 1425-31.

King, R. B., G. M. Raymond, and J. B. Bassingthwaighte. 1996. Modeling blood flow heterogeneity. *Ann Biomed Eng* 24, no. 3: 352-72.

Kwak, D. J., S. D. Kwak, and E. B. Gauda. 2006. The effect of hyperoxia on reactive oxygen species (ros) in rat petrosal ganglion neurons during development using organotypic slices. *Pediatr Res* 60, no. 4: 371-6.

Matute-Bello, G., C. W. Frevert, and T. R. Martin. 2008. Animal models of acute lung injury. *Am J Physiol Lung Cell Mol Physiol* 295, no. 3: L379-99.

Mercer, R. R. and J. D. Crapo. 1987. Three-dimensional reconstruction of the rat acinus. *J Appl Physiol* 63, no. 2: 785-94.

Merker, M. P., S. H. Audi, B. J. Lindemer, G. S. Krenz, and R. D. Bongard. 2007. Role of mitochondrial electron transport complex i in coenzyme q1 reduction by intact pulmonary arterial endothelial cells and the effect of hyperoxia. *Am J Physiol Lung Cell Mol Physiol* 293, no. 3: L809-19.

Merker, M. P., R. D. Bongard, G. S. Krenz, H. Zhao, V. S. Fernandes, B. Kalyanaraman, N. Hogg, and S. H. Audi. 2004. Impact of pulmonary arterial endothelial cells on duroquinone redox status. *Free Radic Biol Med* 37, no. 1: 86-103.

Miller, W. S. 1947. *The lung*. Springfield, IL: Charles C. Thomas.

Motulsky, H. J. and L. A. Ransnas. 1987. Fitting curves to data using nonlinear regression: A practical and nonmathematical review. *Federation of American Societies for Experimental Biology.* 1: 365-374.

Presson, R. G., Jr., J. A. Graham, C. C. Hanger, P. S. Godbey, S. A. Gebb, R. A. Sidner, R. W. Glenny, and W. W. Wagner, Jr. 1995. Distribution of pulmonary capillary red blood cell transit times. *J Appl Physiol* 79, no. 2: 382-8.

Presson, R. G., Jr., T. M. Todoran, B. J. De Witt, I. F. McMurtry, and W. W. Wagner, Jr. 1997. Capillary recruitment and transit time in the rat lung. *J Appl Physiol* 83, no. 2: 543-9.

Randell, S. H., R. R. Mercer, and S. L. Young. 1990. Neonatal hyperoxia alters the pulmonary alveolar and capillary structure of 40-day-old rats. *Am J Pathol* 136, no. 6: 1259-66.

Rich, P. R. and R. Harper. 1990. Partition coefficients of quinones and hydroquinones and their relation to biochemical reactivity. *FEBS Lett* 269, no. 1: 139-44.

Schwab, A. J. and C. A. Goresky. 1996. Hepatic uptake of protein-bound ligands: Effect of an unstirred disse space. *Am J Physiol* 270, no. 5 Pt 1: G869-80.

Singh, C. P., Singh, N., Singh, J., Brar, G.K., Singh, G. 2001. Oxygen therapy. *Journal, Indian Academy of Clinical Medicine* 2, no. 3: 178-84.

Sjostrom, K. and J. D. Crapo. 1983. Structural and biochemical adaptive changes in rat lungs after exposure to hypoxia. *Lab Invest* 48, no. 1: 68-79.

Staub, N. C. and E. L. Schultz. 1968. Pulmonary capillary length in dogs, cat and rabbit. *Respir Physiol* 5, no. 3: 371-8.

Turrens, J. F. 2003. Mitochondrial formation of reactive oxygen species. *J Physiol* 552, no. Pt 2: 335-44.

Turrens, J. F., B. A. Freeman, J. G. Levitt, and J. D. Crapo. 1982. The effect of hyperoxia on superoxide production by lung submitochondrial particles. *Arch Biochem Biophys* 217, no. 2: 401-10.

Valenca Sdos, S., M. L. Kloss, F. S. Bezerra, M. Lanzetti, F. L. Silva, and L. C. Porto. 2007. [effects of hyperoxia on wistar rat lungs]. *J Bras Pneumol* 33, no. 6: 655-62.

Wagner, W. W., Jr., L. P. Latham, M. N. Gillespie, J. P. Guenther, and R. L. Capen. 1982. Direct measurement of pulmonary capillary transit times. *Science* 218, no. 4570: 379-81.

Wagner, W. W., Jr., L. P. Latham, W. L. Hanson, S. E. Hofmeister, and R. L. Capen. 1986. Vertical gradient of pulmonary capillary transit times. *J Appl Physiol* 61, no. 4: 1270-4.

Ware, L. B., Matthay, M.A. 2000. The acute respiratory distress syndrome. The New England Journal of Medicine 342: 1334-49.

Zierhut, M. L., J. C. Gardner, M. E. Spilker, J. T. Sharp, and P. Vicini. 2007. Kinetic modeling of contrast-enhanced mri: An automated technique for assessing inflammation in the rheumatoid arthritis wrist. Ann Biomed Eng 35, no. 5: 781-95.

GLOSSARY OF TERMS

$h_c(t)$ capillary transit time distribution

$C_R(t)$ concentration (1/ml) vs. time (sec) curve of the vascular indicator in the venous effluent at a time t following bolus injection at $t = 0$

$C_F(t)$ concentration (1/ml) vs. time (sec) curve of the flow-limited indicator in the venous effluent at a time t following bolus injection at $t = 0$

$C_{tub}(t)$ concentration (1/ml) vs. time (sec) curve of the vascular indicator in the venous effluent at a time t, following injection with the lung removed from the ventilation-perfusion system

$\bar{t}$ mean transit time (the first moment) (sec)

$\bar{t}_v$ lung vascular mean transit time (sec)

$\bar{t}_c$ capillary mean transit time (sec)

$\bar{t}_R$ mean transit time of the vascular indicator concentration vs. time outflow curve, $C_R(t)$ (sec)

$\bar{t}_F$ mean transit time of the flow-limited indicator concentration vs. time outflow curve, $C_F(t)$ (sec)

$\bar{t}_{tub}$ mean transit time of the tubing concentration vs. time outflow curve, $C_{tub}(t)$ (sec)

$\bar{t}_e$ extravascular mean residence time (sec)

σ^2 variance (second central moment) (sec^2)

σ_v^2 variance of lung total vascular transit times (sec^2)

σ_c^2 variance of $h_c(t)$ (sec^2)

σ_R^2 variance of the vascular indicator concentration versus time outflow curve, $C_R(t)$ (sec^2)

σ_F^2	variance of the flow-limited indicator concentration versus time outflow curve, $C_F(t)$ (sec^2)
σ_e^2	$\sigma_F^2 - \sigma_R^2$, extravascular variance (sec^2)
m^3	skewness (third central moment) (sec^3)
m_c^3	skewness of $h_c(t)$ (sec^3)
m_R^3	skewness of the vascular indicator concentration versus time outflow curve (sec^3)
m_F^3	skewness of the flow-limited indicator concentration versus time outflow curve (sec^3)
Q_v	lung vascular volume (ml)
Q_c	lung capillary volume (ml)
Q_t	tissue volume accessible to the flow-limited indicator from the vascular region (ml)
Q_e	apparent extravascular volume of CoQ_1H_2 (ml)
RD_V	relative dispersion of the vascular transit time distribution
RD_c	relative dispersion of the capillary transit time distribution
F	perfusate flow (ml/min)
M	tissue-to-plasma partition coefficient of the flow-limited indicator
K	indicator-BSA binding equilibrium dissociation constant
D	vessel diameter (m)
P_t	transpulmonary pressure (torr)
α	distensibility coefficient
Hct	circulatory blood hematocrit (%)
P_a	lung perfusion pressure (torr)

BSA	Bovine Serum Albumin (%)
FAPGG	N-[3-(2-Furyl) acryloyl]-Phe-Gly-Gly
FITC-dex	fluorescein isothiocyanate labeled dextran
CoQ_1	coenzyme Q1 (2,3-dimethoxy-5-methyl-6-[3-methyl-2-butenyl]-1,4-benzoquinone)
CoQ_1H_2	coenzyme Q_1 hydroquinone (reduced form of CoQ_1)
DQ	duroquinone
DQH_2	durohydroquinone (reduced form of DQ)
NQO1	NAD(P)H: quinone oxidoreductase 1

APPENDIX A

PERFUSATE COMPOSITION AND COQ$_1$H$_2$ PREPARATION

A.1. Preparation of Perfusate:

Listed below are the steps to prepare 300 ml of perfusate. Perfusate of a different volume can be prepared by scaling the individual ingredients appropriately.

i.   Prepare a bottle of de-ionized water (DH$_2$O).

ii.   Take a 300 ml beaker, label it and place a stirring stick in it. Add 250 ml of DH$_2$O into the beaker (250ml for every 300 ml perfusate).

iii. Place the beaker on a heater on low heat with 'stir' set to 2.

iv.   For every 300 ml BSA, add the following amounts of stock and stuff to the beaker in the order specified below:

   a. Stock
      i.   KCl (Potassium chloride): 1.5 ml
      ii. KH$_2$PO$_4$ (Potassium dihydrogen phosphate): 1.5 ml
      iii. MgSO$_4$ (Magnesium sulphate): 1.5 ml
      iv. CaCl$_2$ (Calcium chloride): 1.5 ml

   b. Other chemicals
      i.   NaCl (Sodium chloride): 2.07 g
      ii. Dextrose: 0.3 ml
      iii. NaHCO$_3$ (Sodium bicarbonate): 0.63 g
      iv. BSA (Bovine serum albumin): 9g, 15g or 30g to obtain perfusate with BSA concentrations of 3%, 5% and 10% respectively

v.   Cover the beaker with parafilm to prevent contamination.

vi.   Keep stirring the mixture till all the BSA is dissolved and you are left with a homogenous solution.

vii. Pour the contents of the beaker into a graduated cylinder to ensure proper volume and empty the solution into a clean saline bottle. Label the bottle with date and contents.

viii. Place the bottle in a warm water bath (37°C) for 10 minutes.

ix. Bubble a gas composition of 21% O_2, 79% N_2 into the warmed perfusate for about 20 minutes to 'blow off' the CO_2. Check the pH using a blood-gas analyzer. Stop bubbling when the pH value approaches 7.4.

x. Bubble air (21% O_2, 7% CO_2, and 72% N_2) into the warmed perfusate to equilibrate at a pH of 7.4.

Gassing the perfusate in the last two steps may take approximately an hour.

A.2. Preparation of CoQ$_1$H$_2$:

Listed below are the steps for preparation of the bolus injectate of CoQ_1H_2 for use in

MID experiments.

i. Prepare CoQ_1 stock by mixing the following ingredients:
   a. CoQ_1: 5 mg
   b. Ethanol (20 mM): 2 ml

ii. Prepare ethylene-diamine-tetra-acetic-acid (EDTA) stock by mixing the following ingredients:
   a. EDTA: 37 mg
   b. DH$_2$O: 1 ml

iii. Prepare CoQ_1H_2 stock by mixing the following ingredients:
   a. CoQ_1 stock: 375 μl
   b. KBH$_4$ (Potassium borohydride): 15 μl

   Allow one hour for the reaction to complete. Then add:
   c. EDTA stock

   Allow 30 minutes for the reaction to complete. The final stock has a concentration of 15.96 mM

iv.   Prepare the final CoQ_1H_2 bolus injectate (0.1 ml) by mixing the following:
   a. CoQ_1H_2 stock: 75 μl
   b. BSA (bovine serum albumin): 925 μl

APPENDIX B

MATHEMATICAL MODEL

B.1. Single capillary element:

The model utilized for this study has been described previously (Audi 1993; Audi et al. 1998; Audi 1998). Briefly, each capillary element consists (Figure B1) of a capillary region and a surrounding extravascular region, with volumes V_c and V_e, respectively. The model assumes the following:

1. The vascular indicator is confined to the capillary region, whereas the flow-limited (diffusible) indicator can diffuse out of the capillary region into the extravascular region.

2. Flow is restricted to the vascular region.

3. Transport in the extravascular region is only by diffusion. Diffusion of both vascular and flow-limited indicators in the direction of flow is negligible as compared to the axial convective transport.

4. With respect to the flow-limited indicator, diffusion equilibrium within the vascular and the extravascular volumes in the direction perpendicular to the flow direction is instantaneous.

Under these assumptions, the spatial and temporal variations in the concentrations of the vascular (R) and flow-limited (D) indicators in the vascular and extravascular regions are described by the following species balance equations:

$$\frac{\partial[R]}{\partial t} + W \frac{\partial[R]}{\partial x} = 0 \qquad \text{(B1)}$$

$$\frac{\partial[D]}{\partial t} + W \left(\frac{V_c}{V_c + V_e} \right) \frac{\partial[D]}{\partial x} = 0 \qquad \text{(B2)}$$

where, $W = L/t_c$ is the average flow velocity within the capillary region, where t_c is the

capillary transit time and $x = 0$ and $x = L$ are the capillary inlet and outlet, respectively.

$R(t,x)$ and $D(t,x)$ are the vascular concentrations of R and D at distance x from the

capillary inlet ($x = 0$) and time t. The initial condition: at $t = 0$, $[R](x,t) = D(x,t) = 0$;

and the boundary condition: at $x = 0$, $[R](x,t) = D(x,t) = C_{in}(t)$, where $C_{in}(t)$ is the
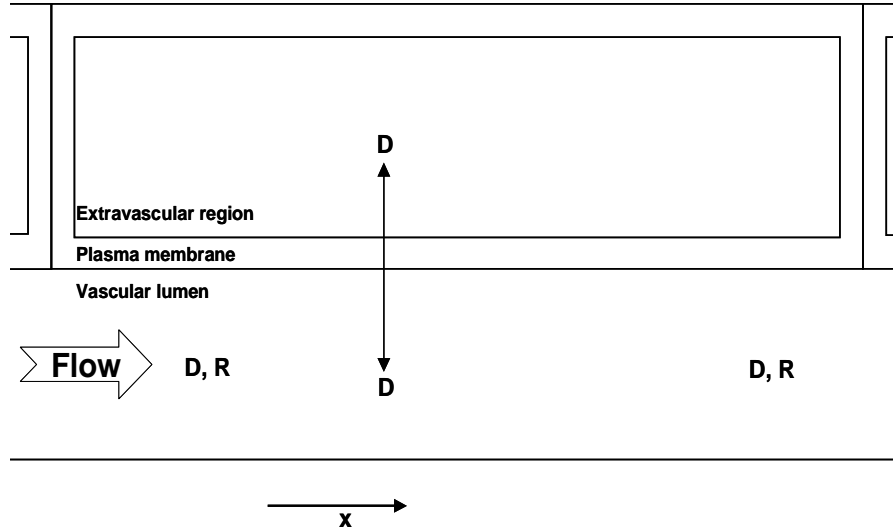
capillary inlet function.

Figure B1: A schematic diagram of a single a capillary element model for the pulmonary disposition of a vascular indicator (R) and a flow-limited indicator (D).

B.2. Whole organ model:

To build a capillary bed or an organ, it is assumed that the capillary bed consists of Nx parallel, non-interacting capillary elements, each possessing a different transit time t_{ci} (Figure B2). These capillary elements differ only in their geometries (i.e., lengths), or flows or combination thereof. However, the per-unit capillary vascular volume, exchange surface area, and physical and chemical properties are the same for all capillary elements. Thus, the capillary bed has a distribution of vascular transit times, $h_c(t)$.
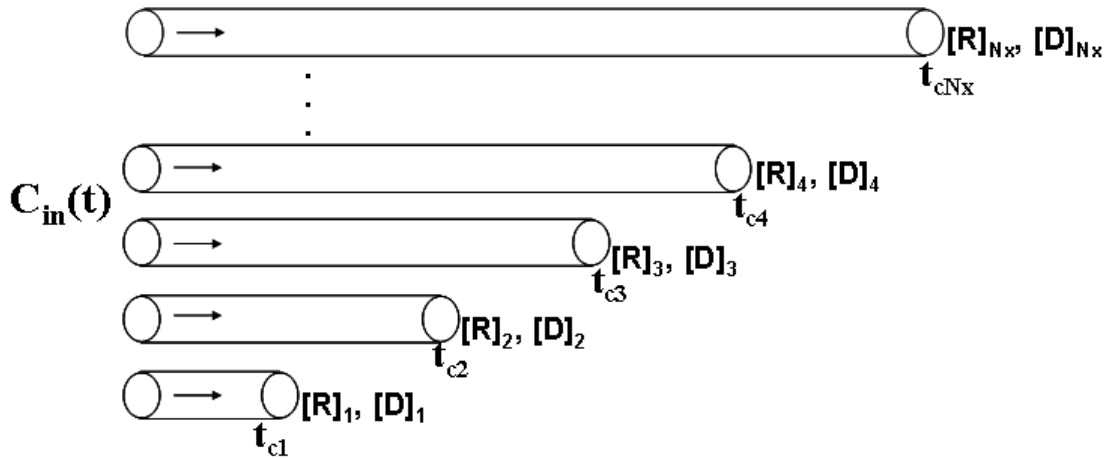

Figure B2: Nx parallel pathways corresponding to the Nx capillaries with different transit times t_{ci}, $i = 1,\ldots$, Nx. $C_{in}(t)$ is the capillary input function. $[R]_i$ and $[D]_i$ are the concentrations of the vascular and flow-limited indicators at the outflow of the ith capillary element.

The organ model assumes random coupling conditions between the conducting vessels and the exchange vessels, i.e., all capillary elements are exposed to the same capillary input $C_{in}(t)$. Given the linearity, commutativity, and associativity of the model, $C_{in}(t)$ could be thought of as the outlet concentration curve that would exist if all arteries and veins were connected directly at a common nexus with no intervening capillaries.

Thus $C_{in}(t)$ would include dispersion from the conducting vessels (i.e., arteries and veins), dispersion as a consequence of any tubing connections involved in the sampling or perfusion system, and dispersion resulting from the injection system. Thus, $C_{in}(t) = (q/F)\, C_{tub}(t) * h_n(t)$ where q is the mass of injected indicator; F is the total flow; $C_{tub}(t)$ is a concentration function representing the mass dispersive processes occurring outside the organ, including the dispersion caused by the injection system; $h_n(t)$ is the transport function for vascular and flow-limited indicators in the conducting vessels of the lung, and * is the convolution operator.

For given values of V_c and $V_e = F.\bar{t}_e$, and a given $h_c(t)$ and $C_{in}(t)$, each represented by a Shifted Random Walk function as previously described, the single capillary element equations (Equations (B1-2)) were solved numerically for each of the Nx capillaries with transit times t_i, i = 1,…, Nx as shown in Figure B2. Then the capillary outflow concentrations for the vascular and flow-limited indicators $C_R(t)$ and $C_F(t)$ were obtained by summing (doing a mass balance on) the outflow concentrations, $[R]_i(t)$ and $[D]_i(t)$, over all Nx capillaries, each capillary outflow being weighed by its corresponding $H_i = \left(\Delta t/2\right)\left(h_c(t_i - \Delta t/2) + h_c(t_i + \Delta t/2)\right)$, which is the flow-weighted fraction of capillaries with transit time t_{ci}, and Δt is the transit time increment. Thus,

$$C_R(t) = \sum_{i=1}^{Nx} H_i\,[R]_i(t) \tag{B3}$$

$$C_D(t) = \sum_{i=1}^{Nx} H_i\,[D]_i(t) \tag{B4}$$